

Scanning probe microscopy of epitaxy of metal complex oxides

Alexander Tselev

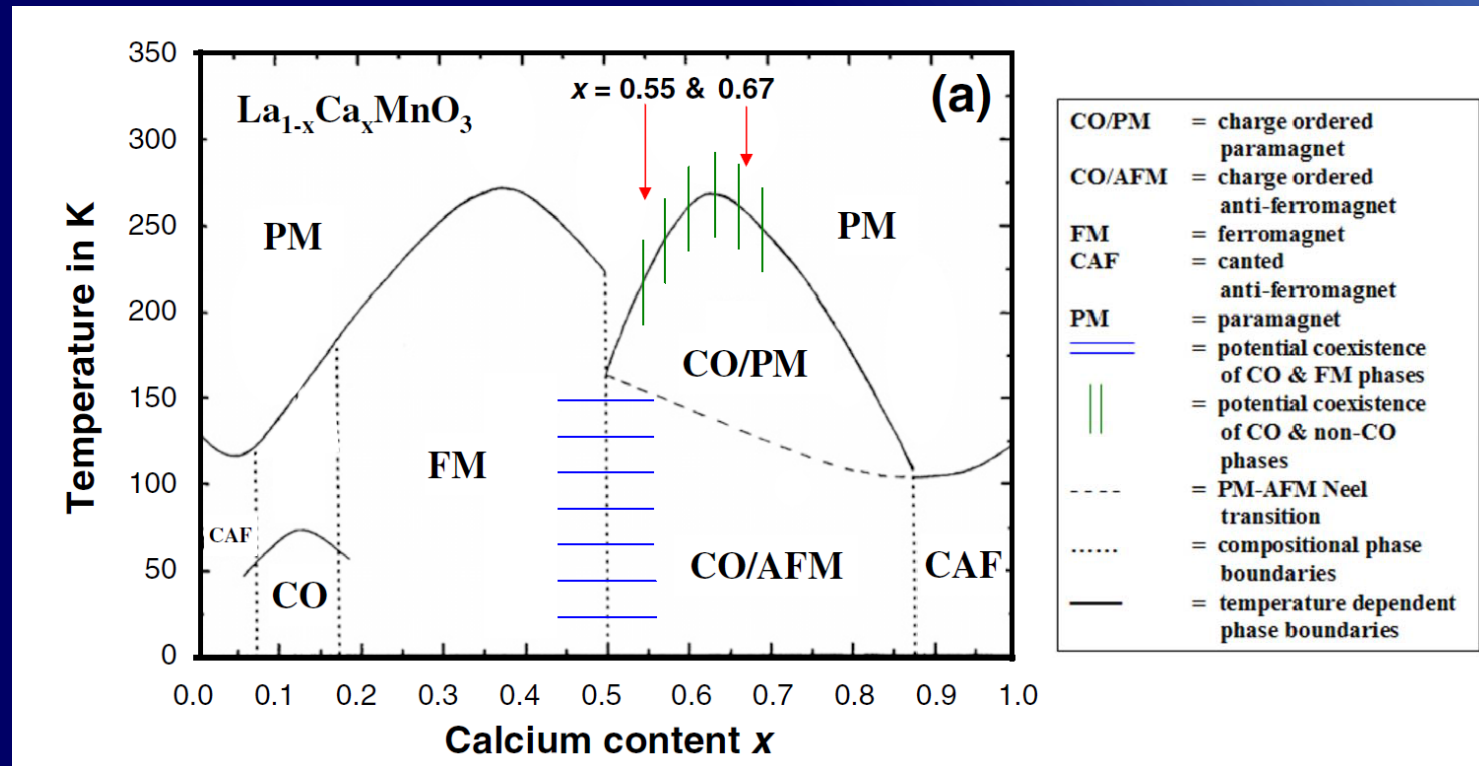
University of Aveiro, Portugal



COMPLEX OXIDES

		1	2	3	4	5	6	7	8	9	10	11	12	13	14	15	16	17	18			
																Phnctogens	Chalcogens	Halogens				
1	H Hydrogen 1.008	<div style="display: flex; justify-content: space-between;"> <div style="width: 15%;"> <p>C Solid</p> <p>Hg Liquid</p> <p>H Gas</p> <p>Rf Unknown</p> </div> <div style="width: 40%; border: 1px solid black; padding: 5px;"> <p style="text-align: center;">Metals</p> <div style="display: flex; justify-content: space-between;"> <div style="width: 15%; border: 1px solid black; padding: 2px;">Alkali metals</div> <div style="width: 15%; border: 1px solid black; padding: 2px;">Alkaline earth metals</div> <div style="width: 15%; border: 1px solid black; padding: 2px;">Lanthanoids</div> <div style="width: 15%; border: 1px solid black; padding: 2px;">Actinoids</div> <div style="width: 15%; border: 1px solid black; padding: 2px;">Transition metals</div> <div style="width: 15%; border: 1px solid black; padding: 2px;">Post-transition metals</div> </div> </div> <div style="width: 15%; border: 1px solid black; padding: 2px;">Metalloids</div> <div style="width: 15%; border: 1px solid black; padding: 2px;">Nonmetals</div> </div>																	2	He Helium 4.0026		
2	Li Lithium 6.94	Be Beryllium 9.0122															B Boron 10.81	C Carbon 12.011	N Nitrogen 14.007	O Oxygen 15.999	F Fluorine 18.998	Ne Neon 20.180
3	Na Sodium 22.990	Mg Magnesium 24.305															Al Aluminium 26.982	Si Silicon 28.085	P Phosphorus 30.974	S Sulfur 32.06	Cl Chlorine 35.45	Ar Argon 39.948
4	K Potassium 39.098	Ca Calcium 40.078	Sc Scandium 44.956	Ti Titanium 47.867	V Vanadium 50.942	Cr Chromium 51.996	Mn Manganese 54.938	Fe Iron 55.845	Co Cobalt 58.933	Ni Nickel 58.693	Cu Copper 63.546	Zn Zinc 65.38	Ga Gallium 69.723	Ge Germanium 72.630	As Arsenic 74.922	Se Selenium 78.971	Br Bromine 79.904	Kr Krypton 83.798				
5	Rb Rubidium 85.468	Sr Strontium 87.62	Y Yttrium 88.906	Zr Zirconium 91.224	Nb Niobium 92.906	Mo Molybdenum 95.95	Tc Technetium (98)	Ru Ruthenium 101.07	Rh Rhodium 102.91	Pd Palladium 106.42	Ag Silver 107.87	Cd Cadmium 112.41	In Indium 114.82	Sn Tin 118.71	Sb Antimony 121.76	Te Tellurium 127.60	I Iodine 126.90	Xe Xenon 131.29				
6	Cs Caesium 132.91	Ba Barium 137.33	57–71 89–103 6 7	Hf Hafnium 178.49	Ta Tantalum 180.95	W Tungsten 183.84	Re Rhenium 186.21	Os Osmium 190.23	Ir Iridium 192.22	Pt Platinum 195.08	Au Gold 196.97	Hg Mercury 200.59	Tl Thallium 204.38	Pb Lead 207.2	Bi Bismuth 208.98	Po Polonium (209)	At Astatine (210)	Rn Radon (222)				
7	Fr Francium (223)	Ra Radium (226)		Rf Rutherfordium (267)	Db Dubnium (268)	Sg Seaborgium (269)	Bh Bohrium (270)	Hs Hassium (277)	Mt Meitnerium (278)	Ds Darmstadtium (281)	Rg Roentgenium (282)	Cn Copernicium (285)	Nh Nihonium (286)	Fl Flerovium (289)	Mc Moscovium (290)	Lv Livermorium (293)	Ts Tennessine (294)	Og Oganesson (294)				
		For elements with no stable isotopes, the mass number of the isotope with the longest half-life is in parentheses.																				
		La Lanthanum 138.91	Ce Cerium 140.12	Pr Praseodymium 140.91	Nd Neodymium 144.24	Pm Promethium (145)	Sm Samarium 150.36	Eu Europium 151.96	Gd Gadolinium 157.25	Tb Terbium 158.93	Dy Dysprosium 162.50	Ho Holmium 164.93	Er Erbium 167.26	Tm Thulium 168.93	Yb Ytterbium 173.05	Lu Lutetium 174.97						
		Ac Actinium (227)	Th Thorium 232.04	Pa Protactinium 231.04	U Uranium 238.03	Np Neptunium (237)	Pu Plutonium (244)	Am Americium (243)	Cm Curium (247)	Bk Berkelium (247)	Cf Californium (251)	Es Einsteinium (252)	Fm Fermium (257)	Md Mendelevium (258)	No Nobelium (259)	Lr Lawrencium (266)						

Phase diagram with phase coexistence



R. Schmidt, Phys. Rev. B 77, 205101 (2008)

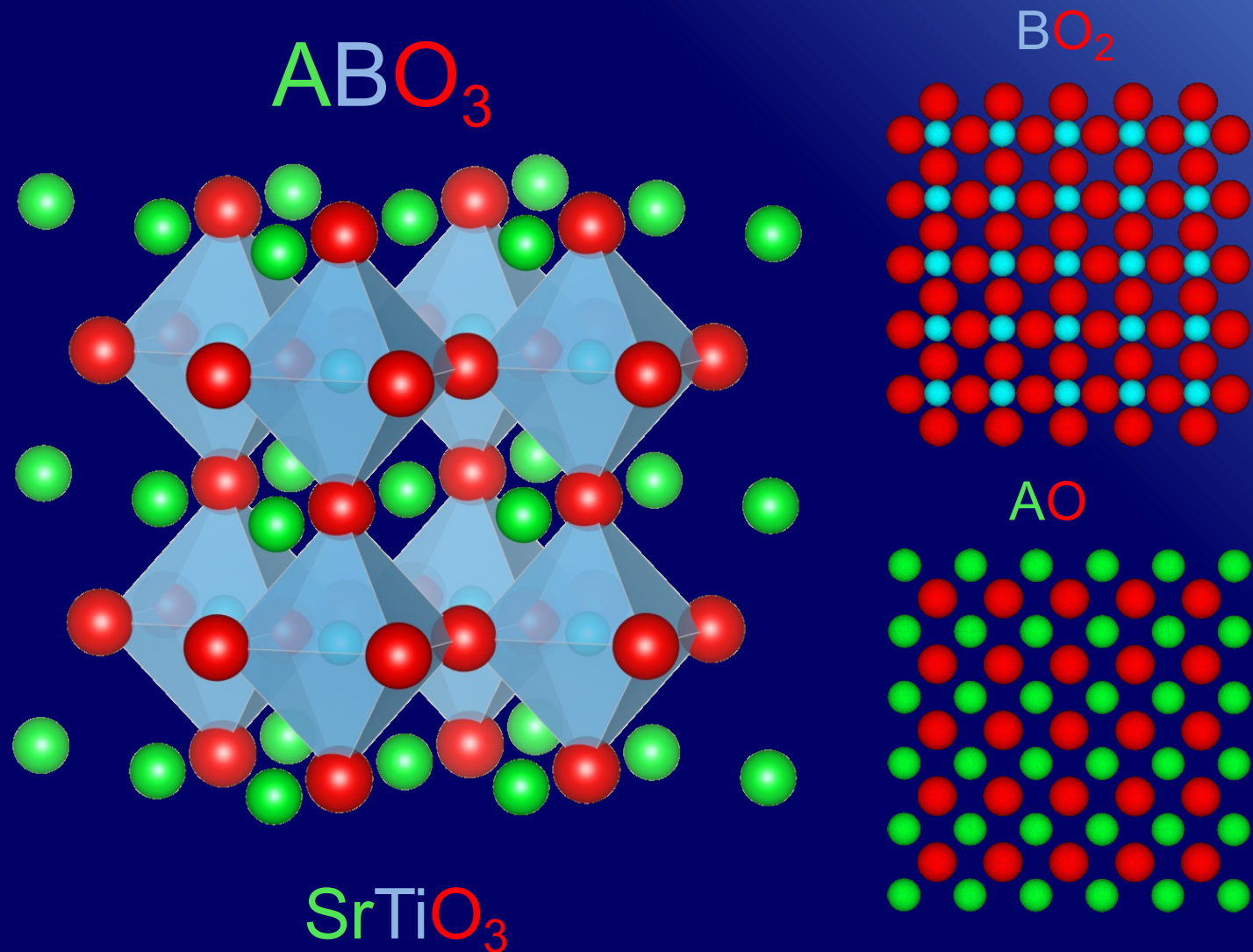
What complex oxides offer

- Superconductivity
- Colossal magnetoresistance
- Ferromagnetism (spintronics)
- Ferroelectricity
- Multiferroism
- Metal-insulator transitions
- Tunability by strain
- Memristive behavior

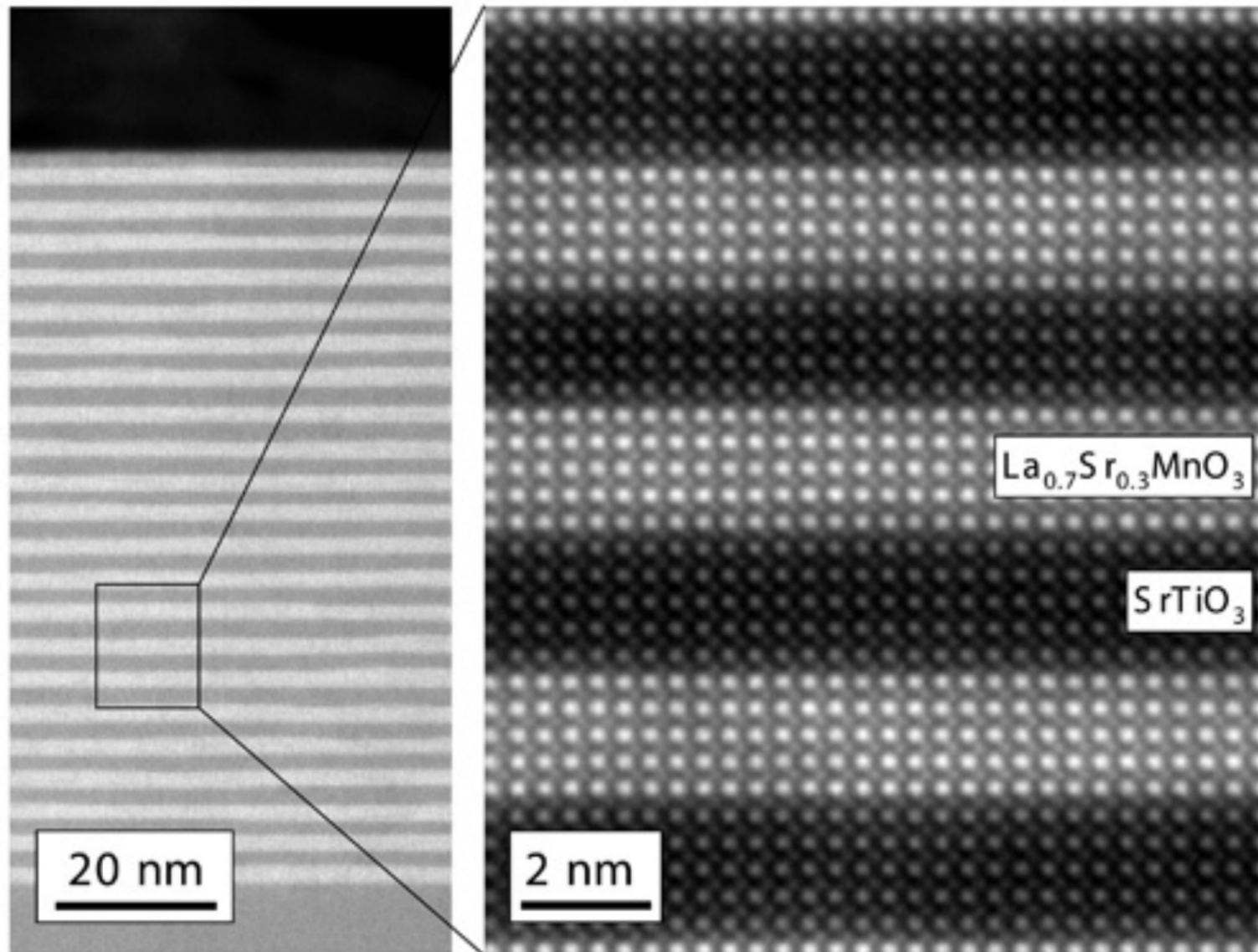
Can be integrated with existing Si-based technologies

- Use in electrochemical energy storage and conversion systems

Perovskite structure



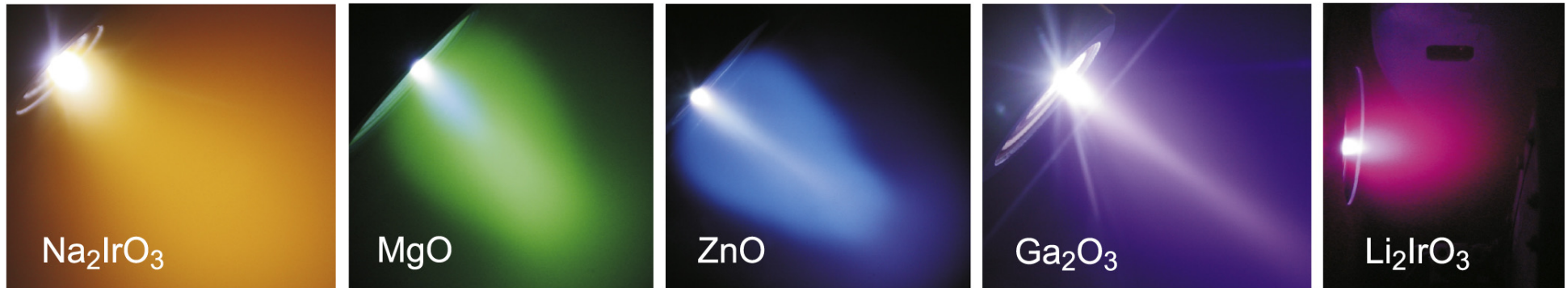
Structure example: LSMO/STO superlattice



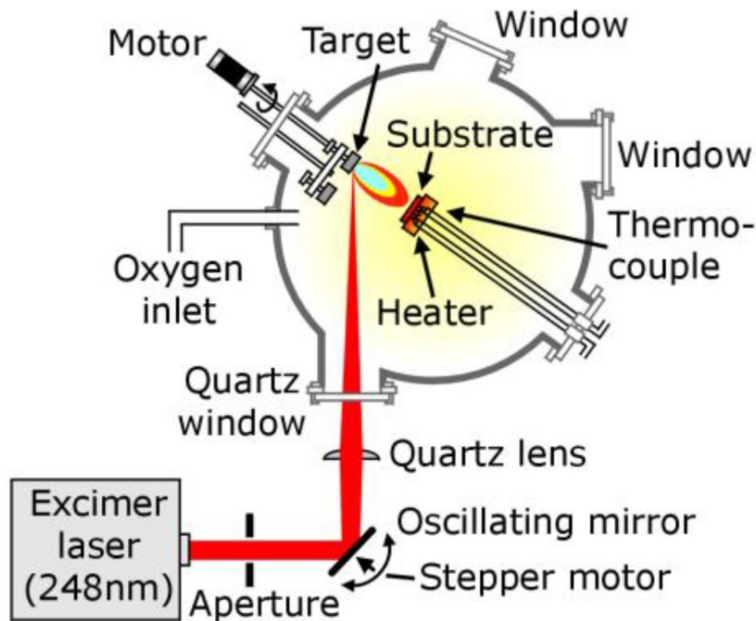
The structure was made using Pulsed Laser Deposition

PULSED LASER DEPOSITION

Pulsed laser deposition



Michael Lorenz et al Semicond. Sci. Technol. (2015)



At peak of laser pulse, temperatures on target can reach $>10^5$ K (> 40 eV!)
Electric fields $> 10^5$ V/cm
Plasma temperatures are 3000-5000 K
Ablated species are with energies 1 –100 eV (thermalization with a background gas)

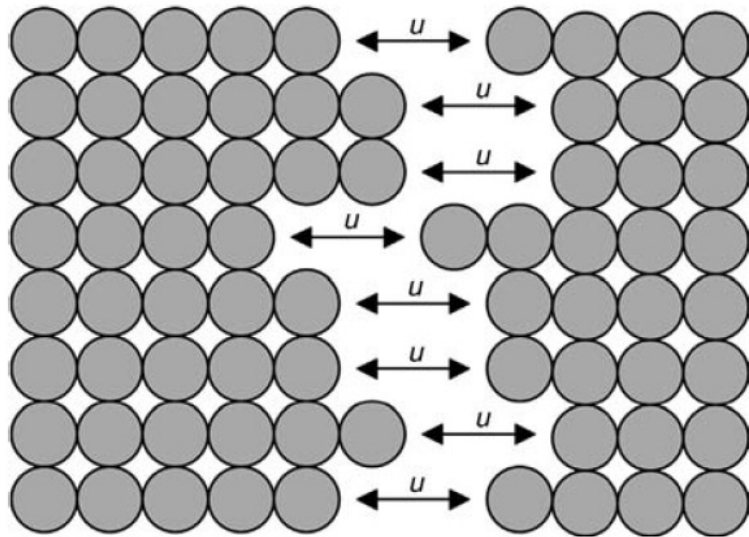


Substrate heating is used to promote adatom mobility and chemical reactions on the surface.

wikipedia.org

SURFACE ENERGY

Surface energy

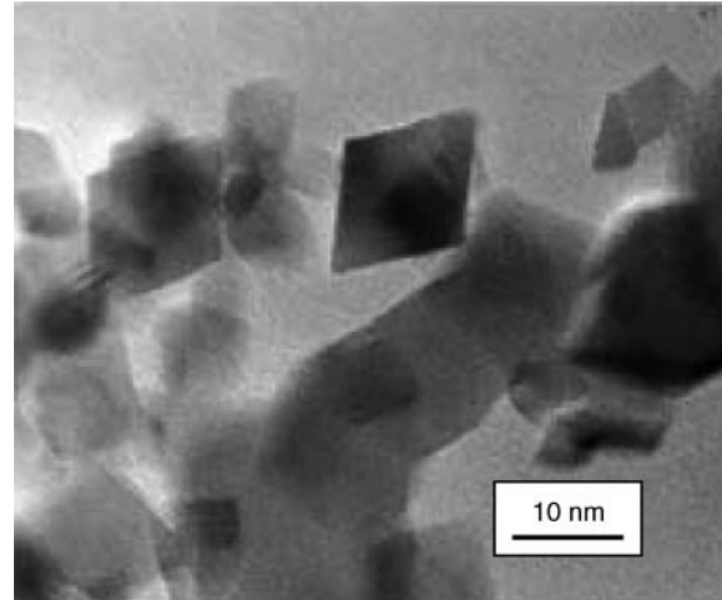


Gibb's energy with account of the surface energy term:

$$G = U - TS + \underline{\gamma}A, \text{ where}$$

γ is the surface energy per unit area

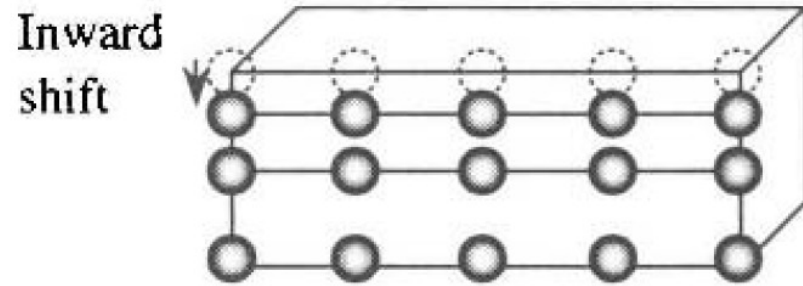
A is the surface area



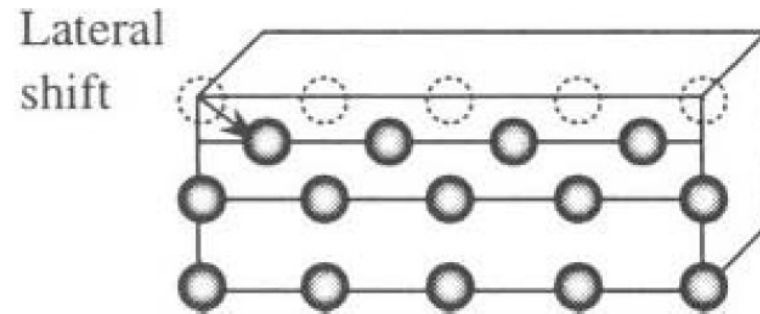
Facetted ceria (CeO₂) nanoparticles.

Note: *amorphous* particles are round!

Surface energy reduction mechanisms



relaxation



reconstruction

- *Due to the force of unbroken bonds, atoms shift towards inside of the crystal*

Surface reconstruction

Changes in bond length and interatomic arrangement on the surface

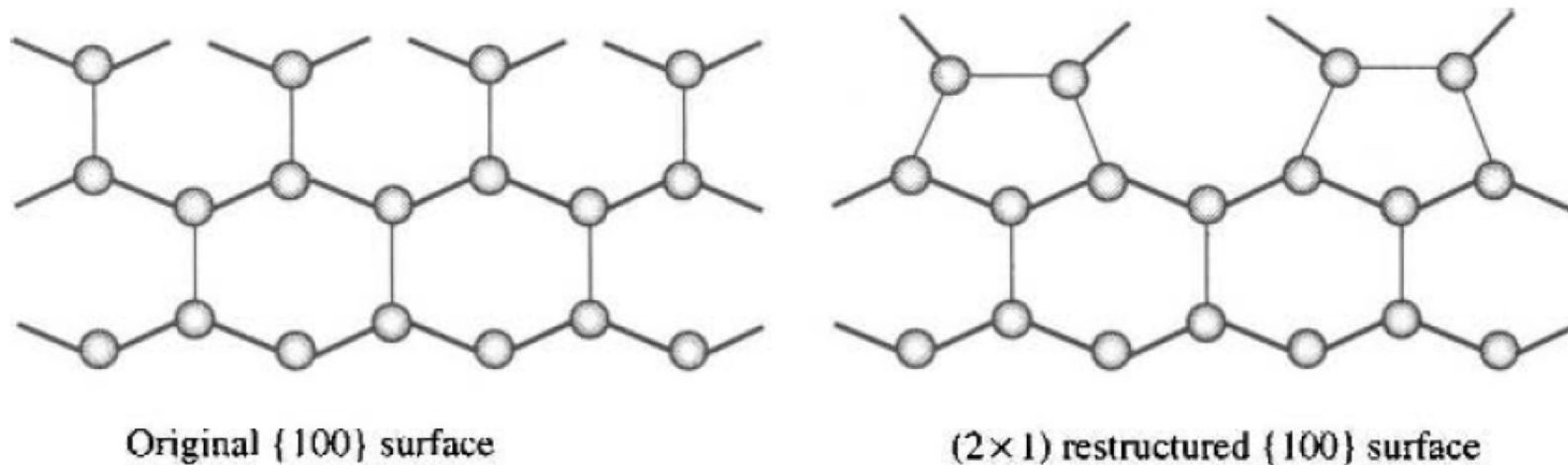
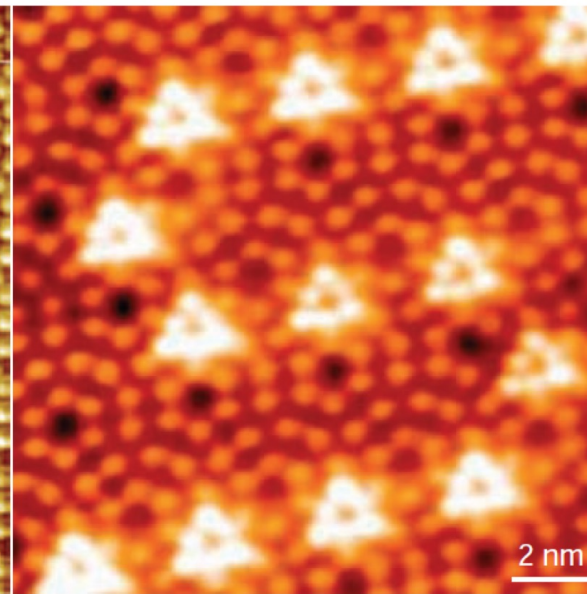
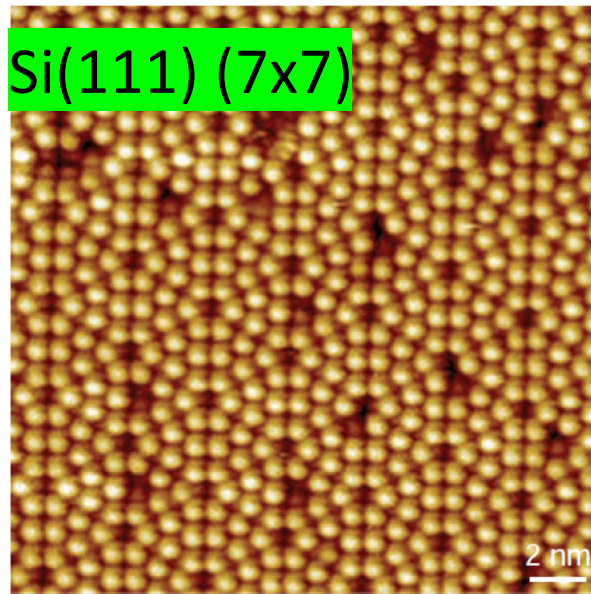


Fig. 2.5. Schematic illustrating the (2×1) restructure of silicon {100} surface.

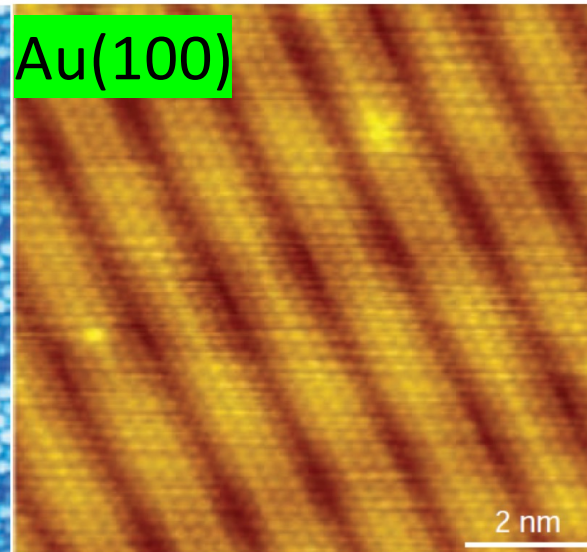
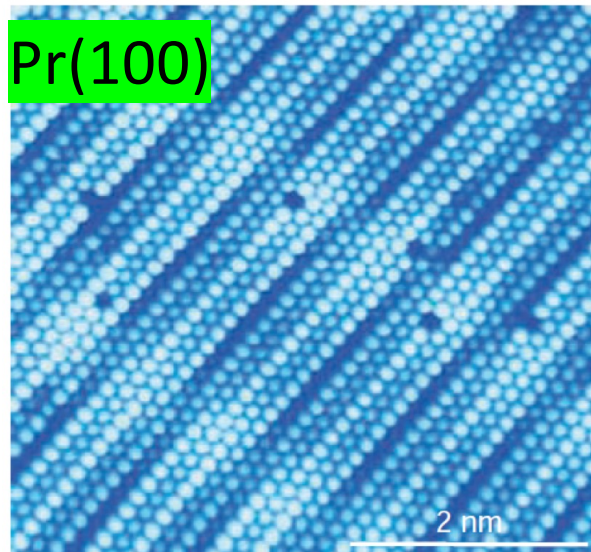
- Material properties are altered due to the presence of the surface up to a depth of a few interatomic distances: 0.5-1.5 nm

Surface reconstructions



Omicron
NanoTechnology GmbH
(<http://www.omicron.de>)

Phys. Rev. Lett . 88 (2002),
066101.

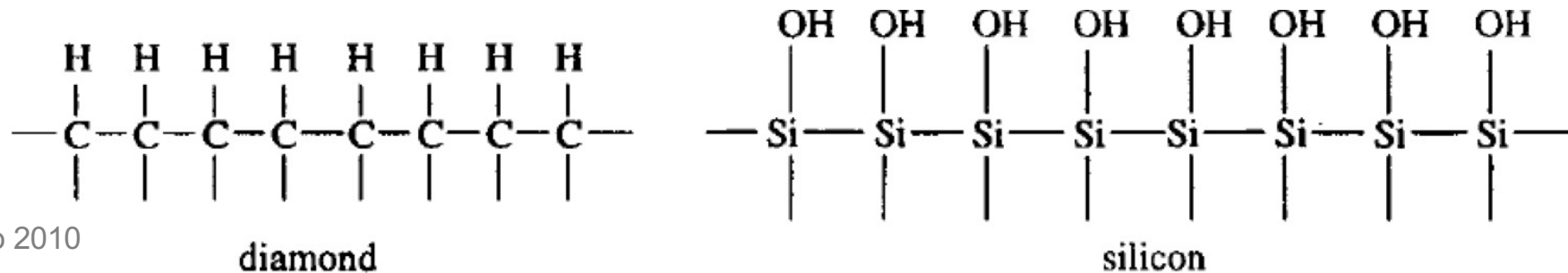


Surf. Sci . 306
(1994), 10–20

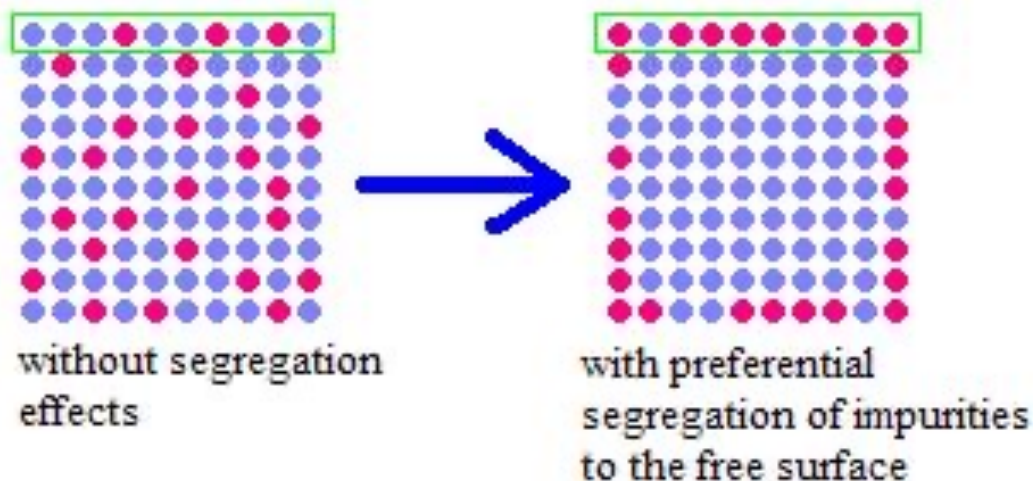
http://en.wikipedia.org/wiki/Scanning_tunneling_microscope

Surface adsorption and composition segregation

- surface adsorption through *chemical* or *physical* adsorption (from a gas of liquid):
 - forming chemical bonds or
 - weak attraction forces such as electrostatic or van der Waals forces



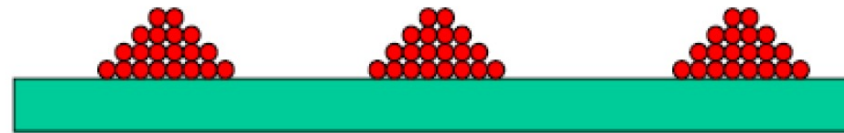
- composition segregation: dopant or impurity enrichment on the surface through solid-state diffusion (from a solid solution)



- Indirect evidences of “surface segregation” in nanomaterials: difficult to dope, and nearly perfect crystal lattice.

Nucleation and growth modes

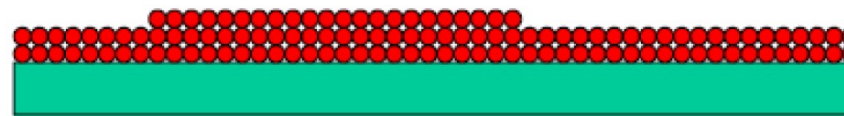
(1) Volmer-Weber: (island growth):



$$\gamma_{sv} < \gamma_{fs} + \gamma_{fv}$$

M. Volmer and A. Weber, *Z. Phys. Chem.* **119**, p. 277 (1926).

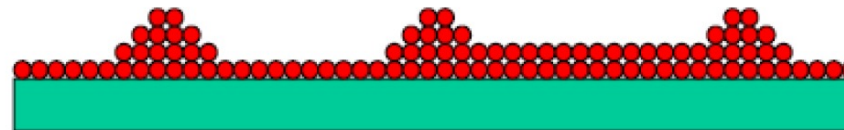
(2) Frank-Van der Merwe: (layer growth; ideal epitaxy):



$$\gamma_{sv} \geq \gamma_{fs} + \gamma_{fv}$$

F. C. Frank and J. H. Van der Merwe, *Proc. R. Soc. London, Ser. A* **198**, p. 205 (1949).

(3) Stranski-Krastanov: (layers + islands):



$$\gamma_{sv} \approx \gamma_{fs} + \gamma_{fv}$$

J. N. Stranski and L. Krastanov, *Ber. Akad. Wiss. Wien* **146**, p. 797 (1938).

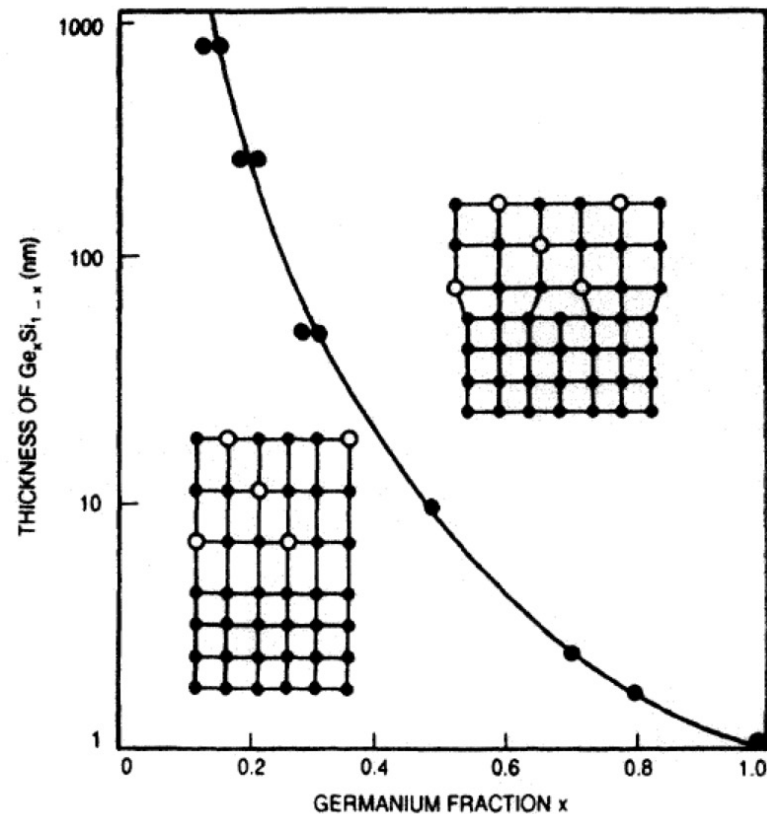
Growth modes in PVD epitaxy



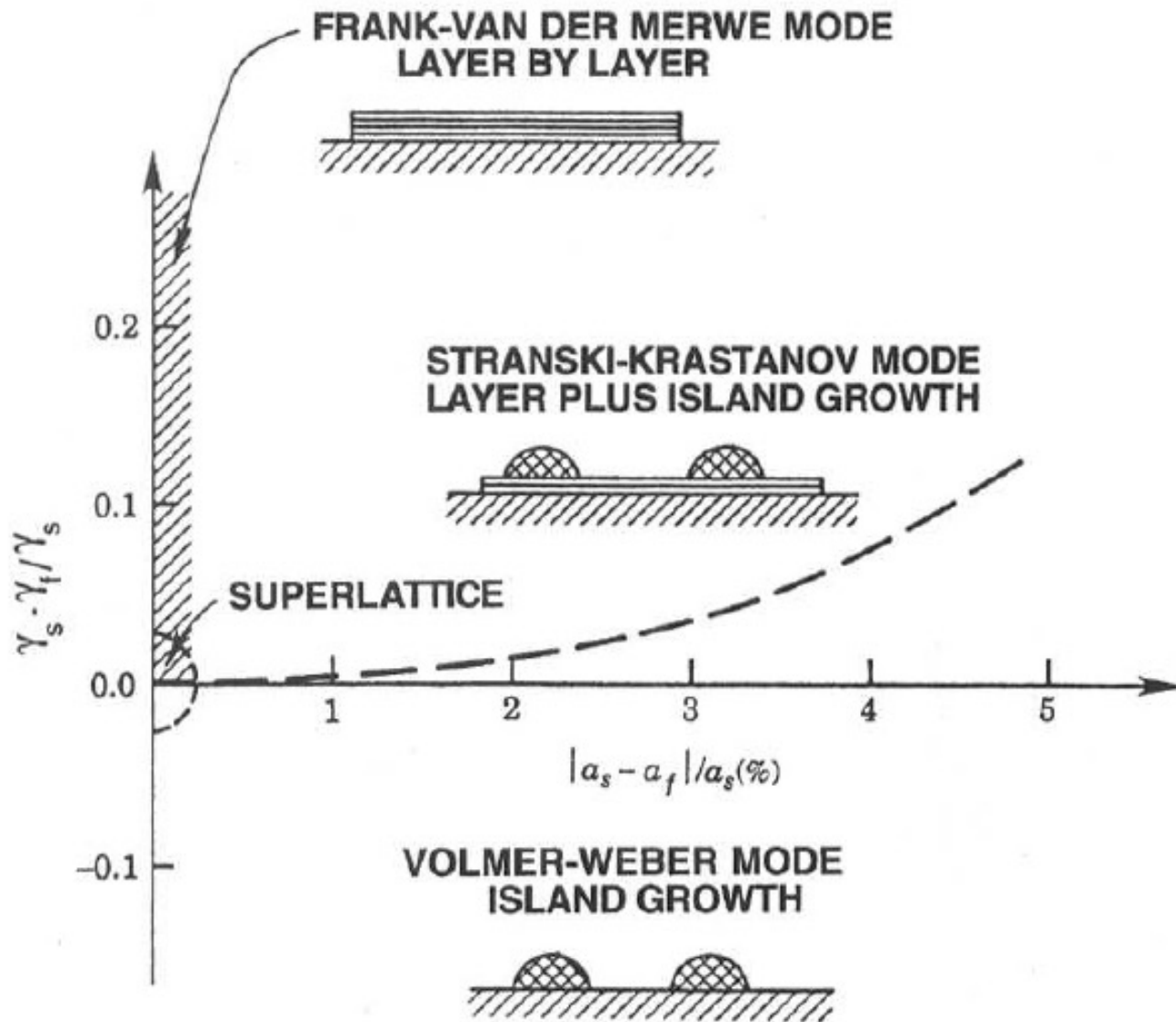
Lattice misfit

$$f = \frac{a_{s0} - a_{f0}}{a_{f0}} = \frac{\Delta a_0}{a_0}$$

$a_{0s,f}$ are unstrained lattice parameters of substrate and film



Thermodynamic aspects



A set of available substrates for perovskite oxides

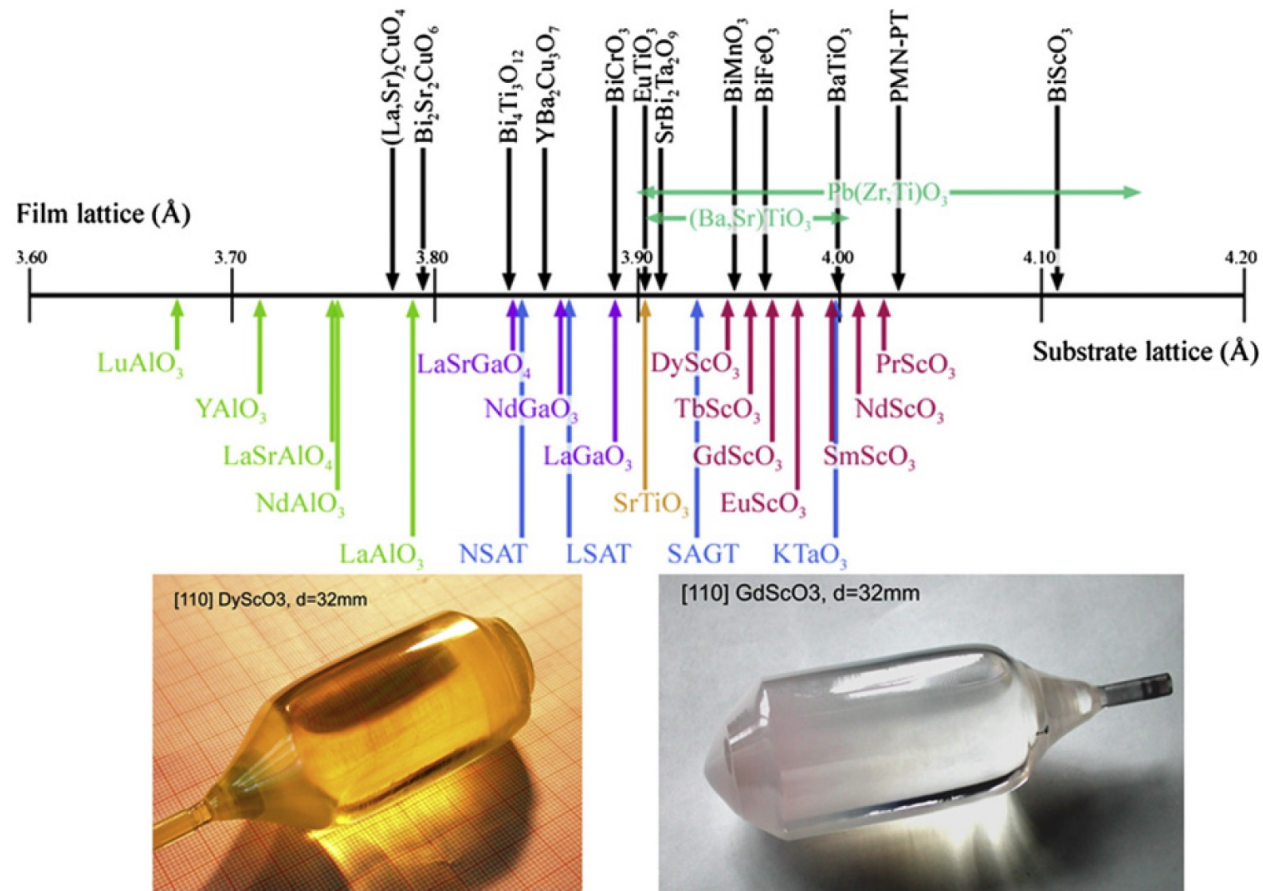
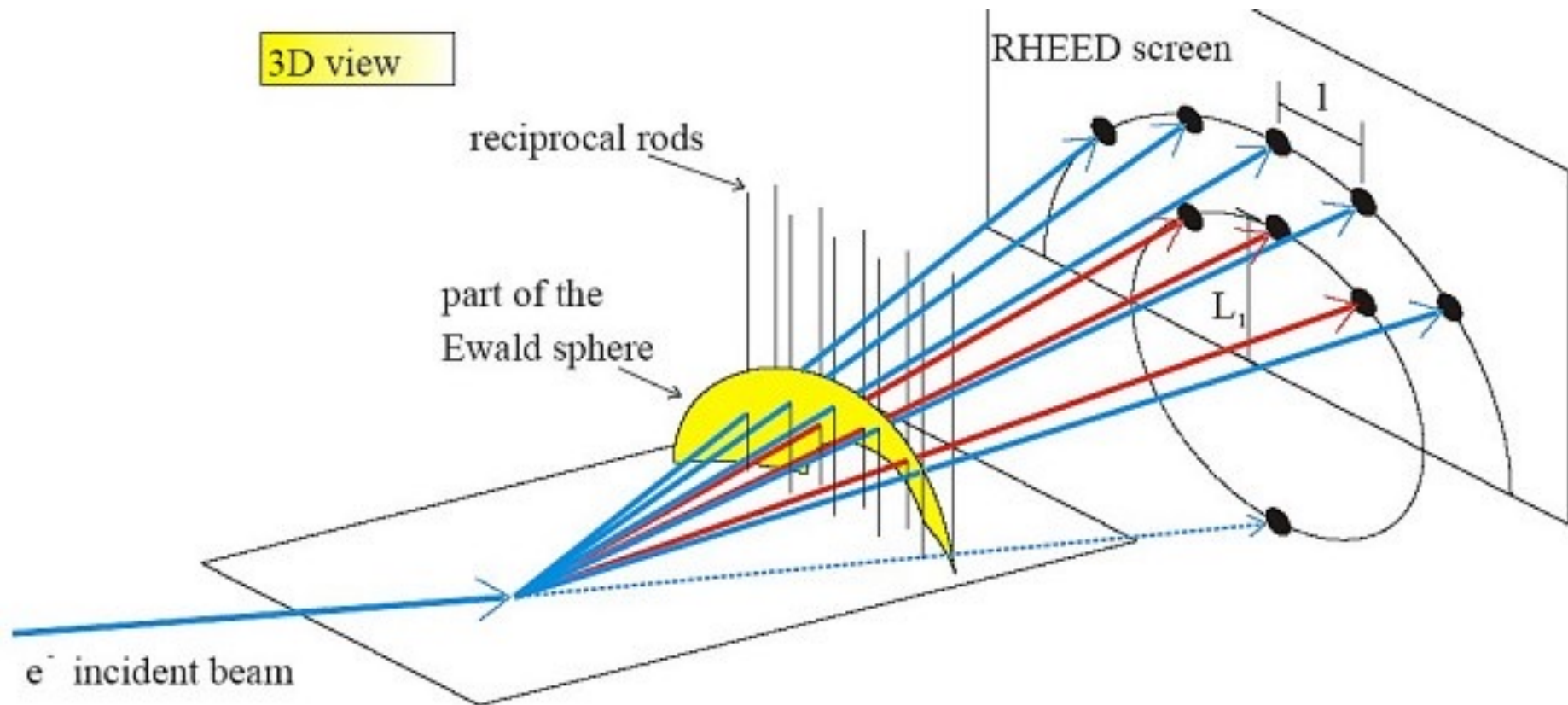


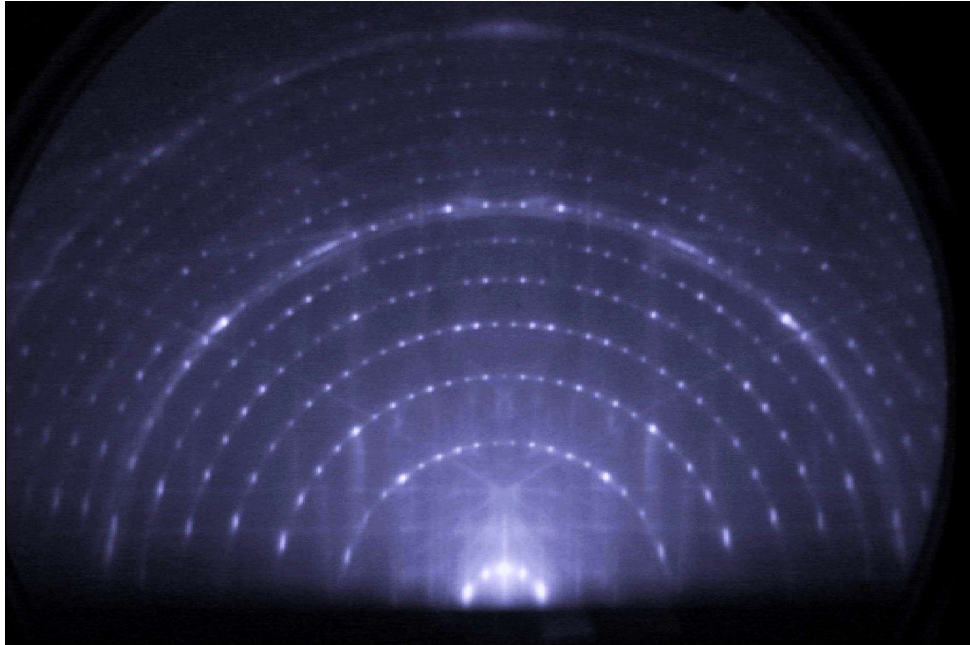
Fig. 3. A number line showing the pseudotetragonal or pseudocubic a -axis lattice constants in angstroms of some perovskites and perovskite-related phases of interest including multiferroics (above the number line) and of some of the perovskite and perovskite-related substrates that are available commercially (below the number line). The photos of exemplary single crystals used as substrates are from Ref. [96].

REFLECTION HIGH-ENERGY ELECTRON DIFFRACTION

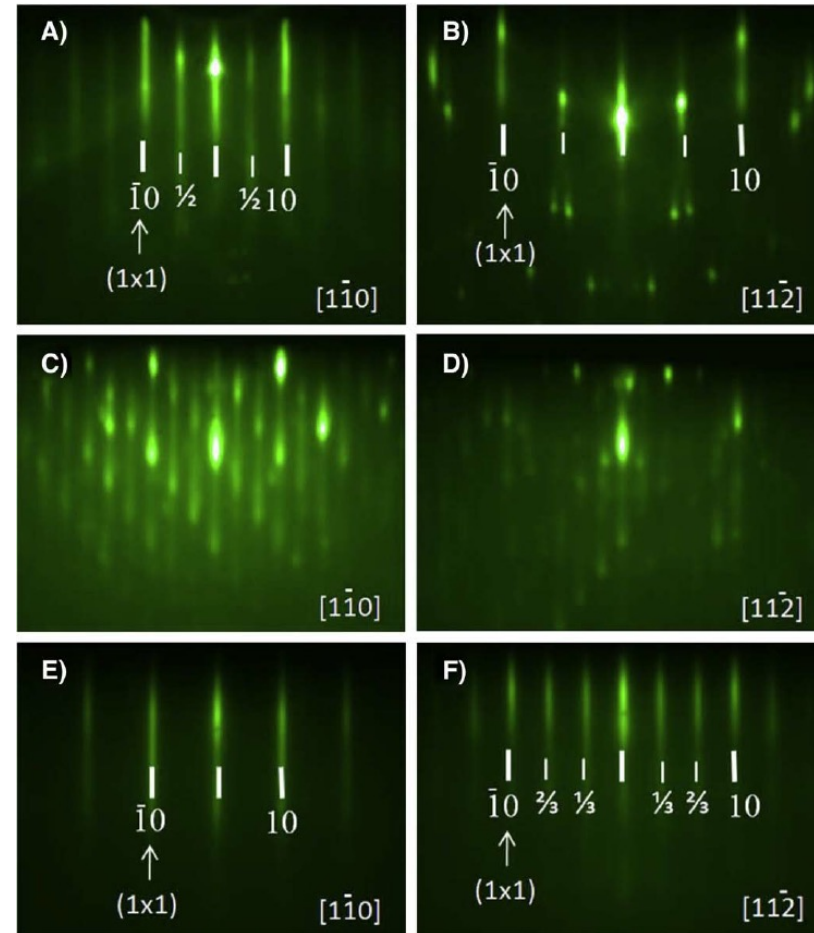
Reflection High-Energy Electron Diffraction (RHEED)



Example: RHEED patterns



<http://nano.umcs.lublin.pl/en-RHEED.php>

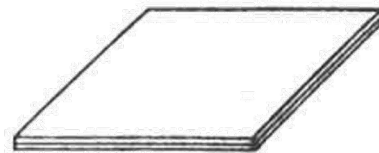
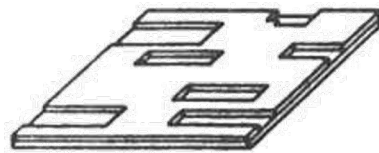
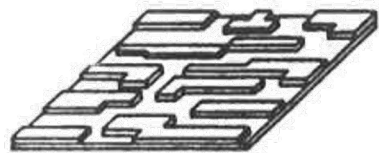
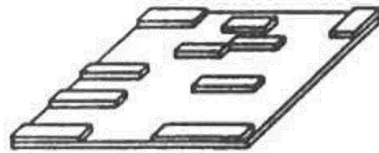
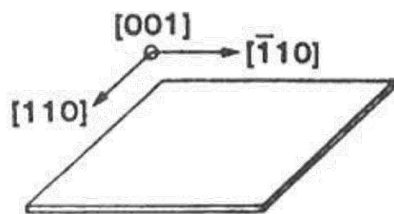


S. Olive-Mendez et al. *Thin Solid Films* (2008)

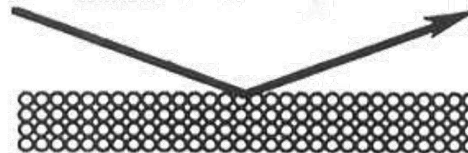
In situ control of film growth

Reflection High-Energy Electron Diffraction

MONOLAYER GROWTH



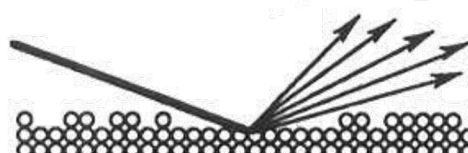
ELECTRON BEAM



$\bar{\theta} = 0$



$\bar{\theta} = 0.25$



$\bar{\theta} = 0.5$

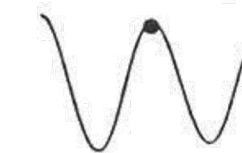
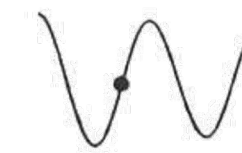
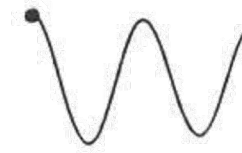


$\bar{\theta} = 0.75$

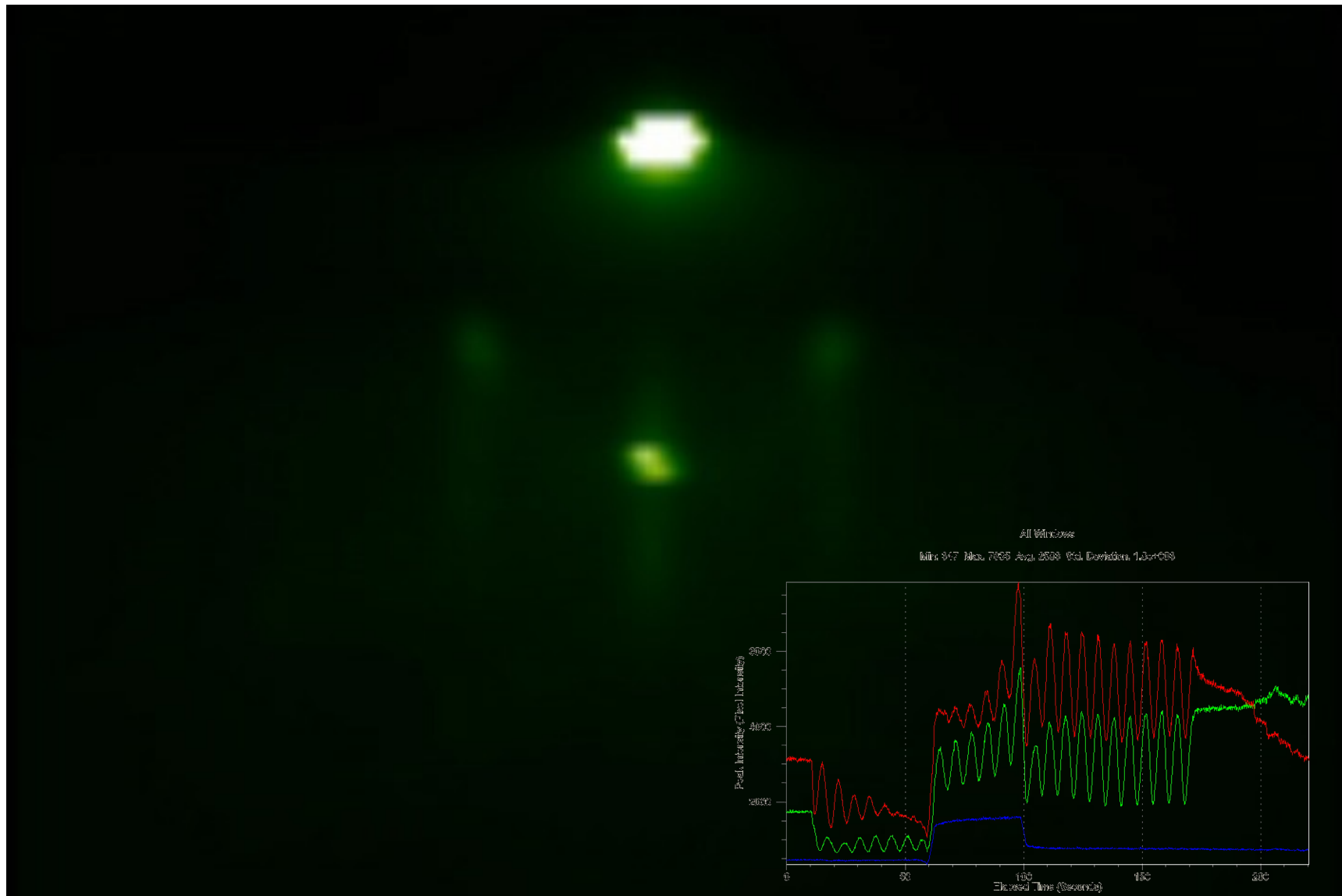


$\bar{\theta} = 1.0$

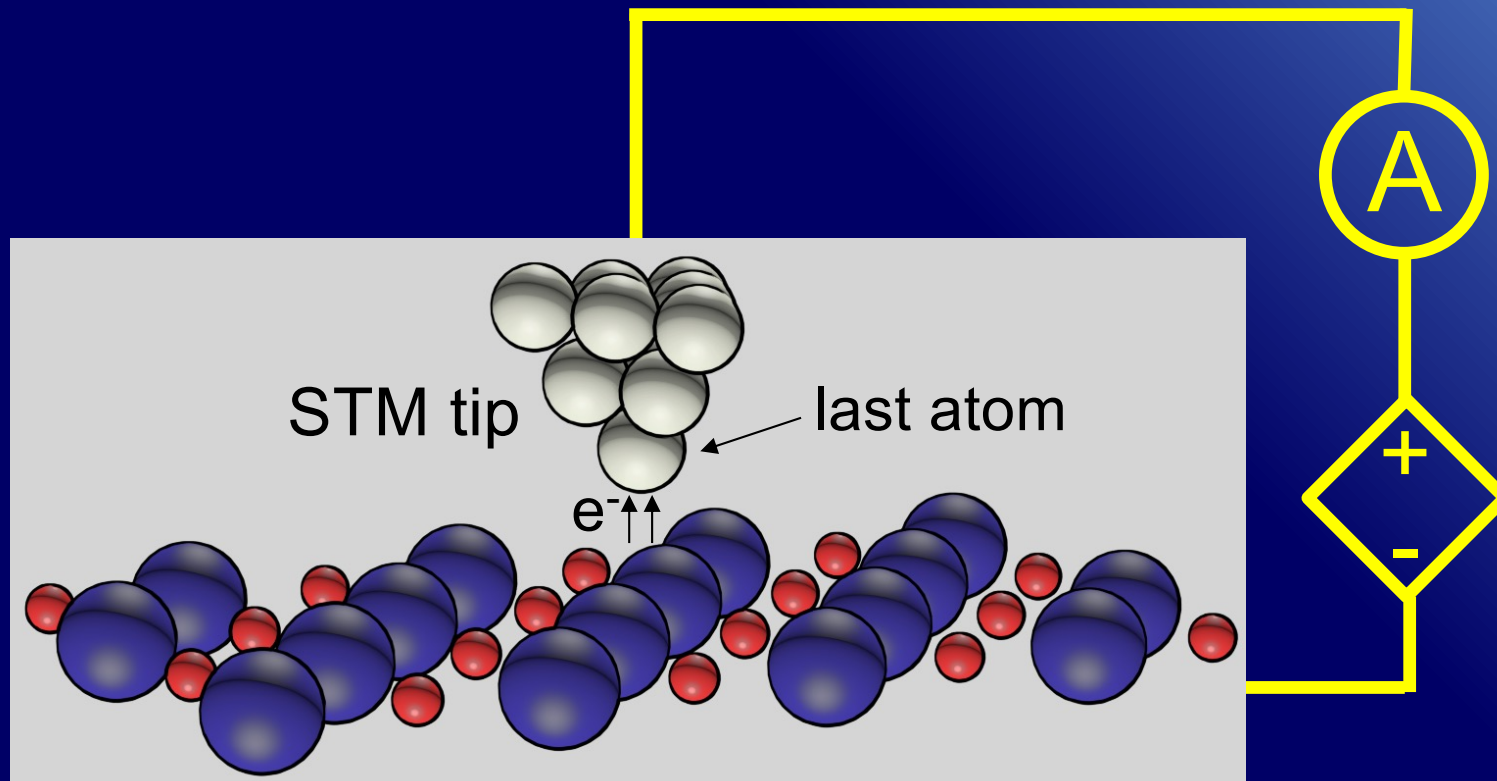
RHEED SIGNAL



RHEED during a real deposition

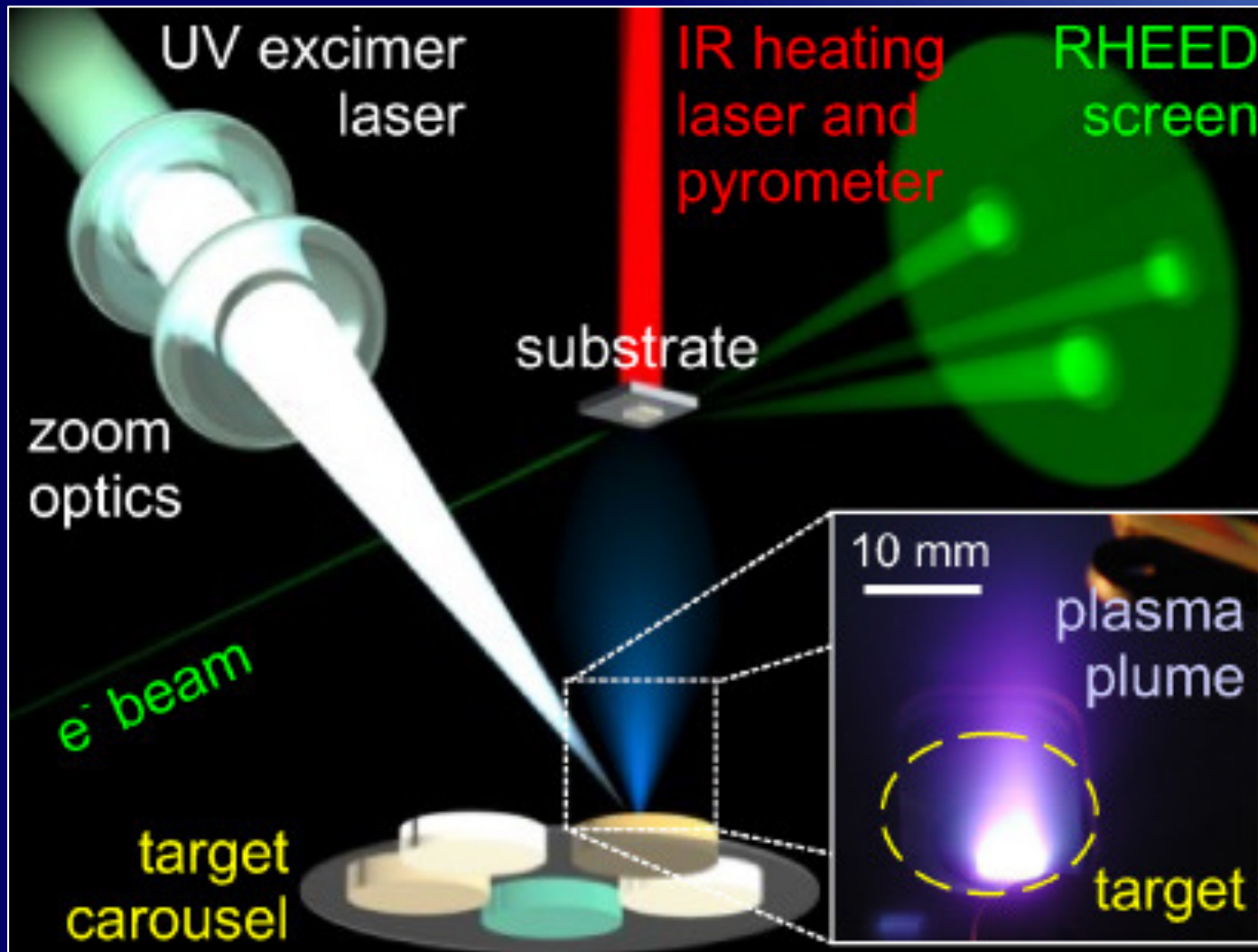


Scanning tunneling microscopy



- *Atomic* resolution is generally *very difficult* to achieve on PLD-grown films

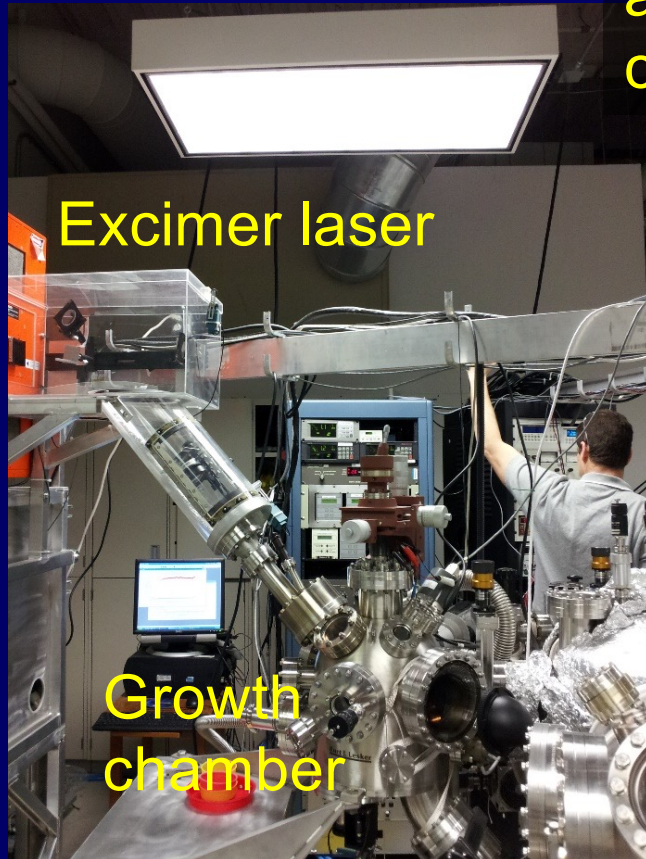
Pulsed Laser Deposition



The schematic is from: M. Opel, J. Phys. D 45, 033001 (2012)

NanoTransport system at CNMS

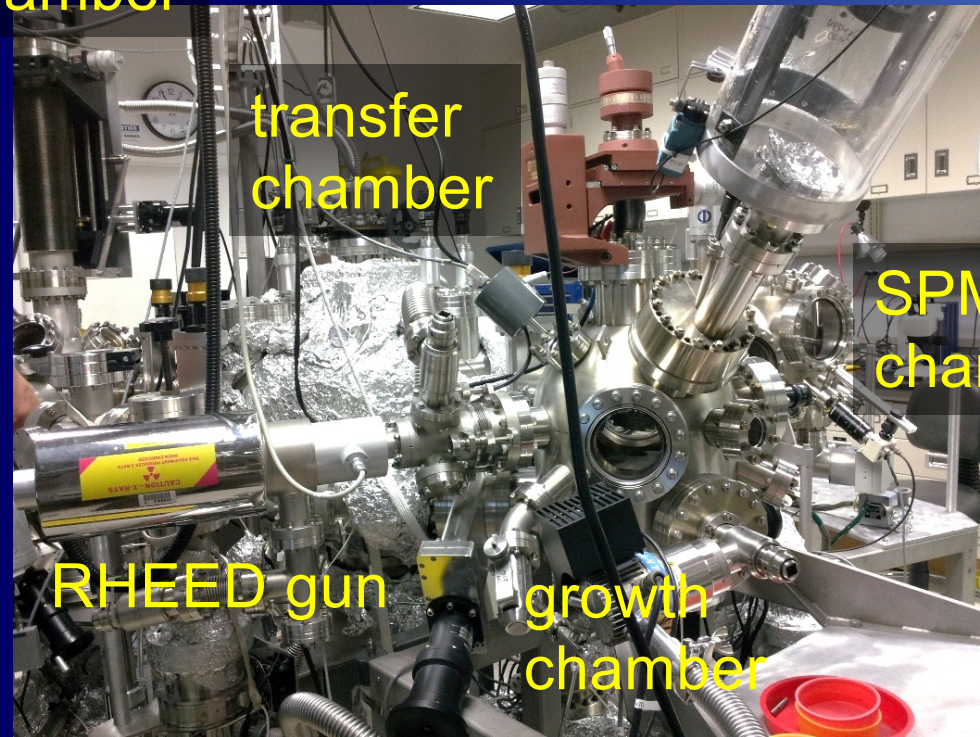
<http://www.cnms.ornl.gov>



Excimer laser

Growth chamber

analysis chamber



transfer chamber

RHEED gun

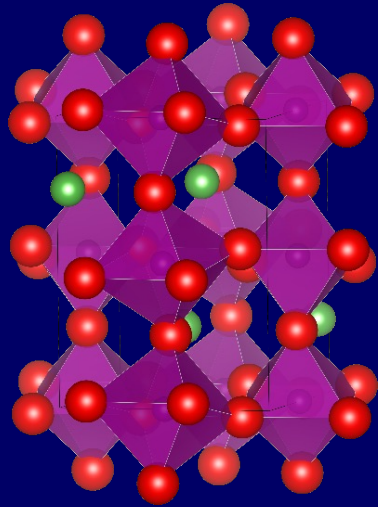
growth chamber

SPM chamber

STM
AFM
in
UHV

Epitaxial film growth

LaMnO₃

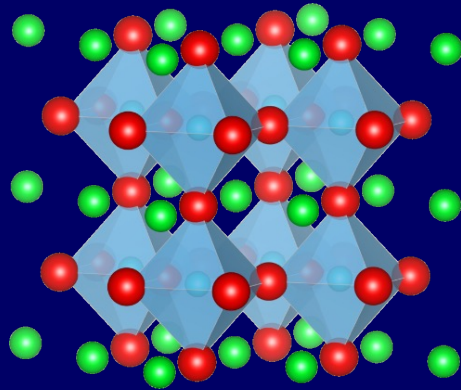


Growth at:
elevated substrate temperatures
650-850 °C &
in oxygen atmosphere 1-300 mTorr

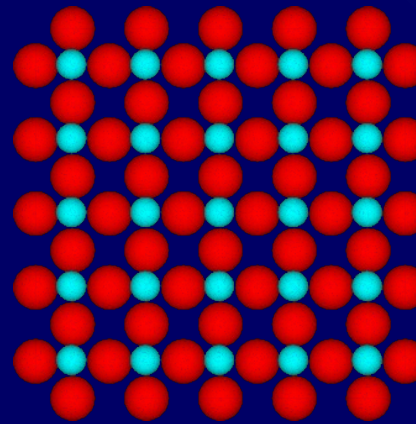
B-terminated single-crystalline substrate

BO₂

SrTiO₃



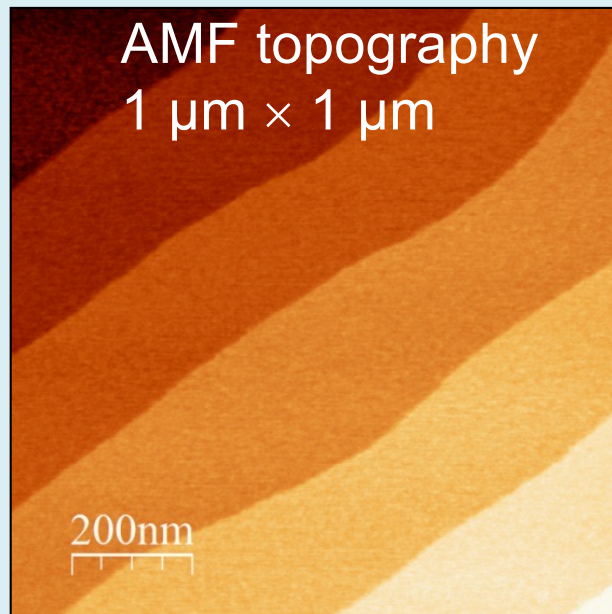
substrate





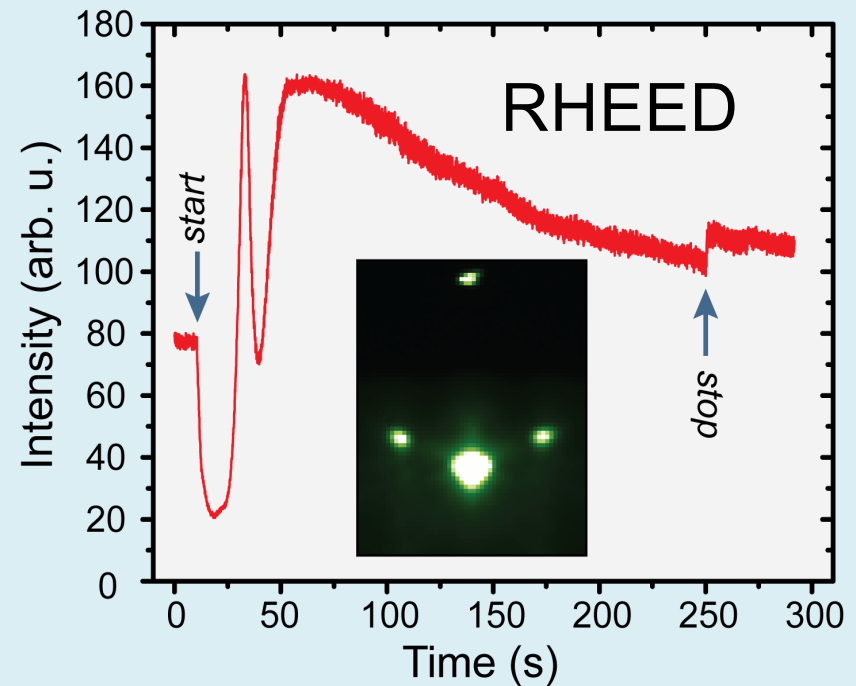
Widely used as a metal electrode

Film growth



RMS Roughness = 55 pm

Substrate selection:
RMS roughness < 70 pm

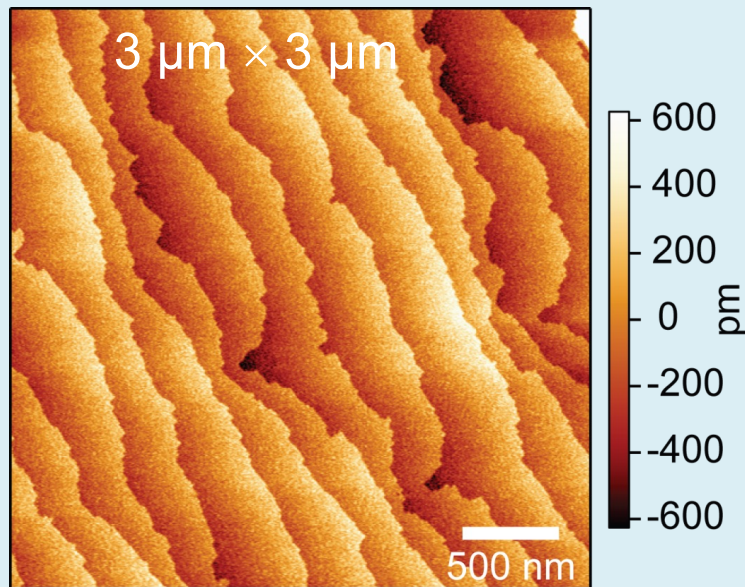


Growth modes:

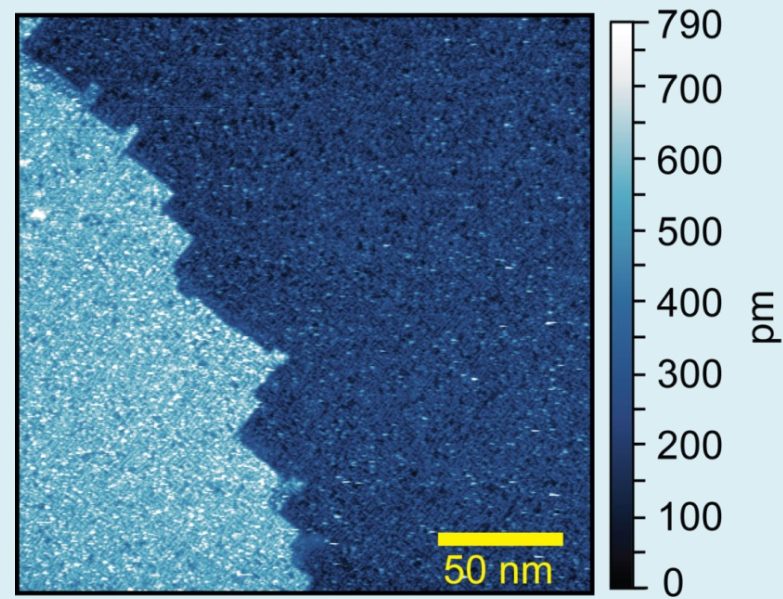
- 690 °C – step-flow
- 650°C – step-flow/island-formation

Film surface: larger scale

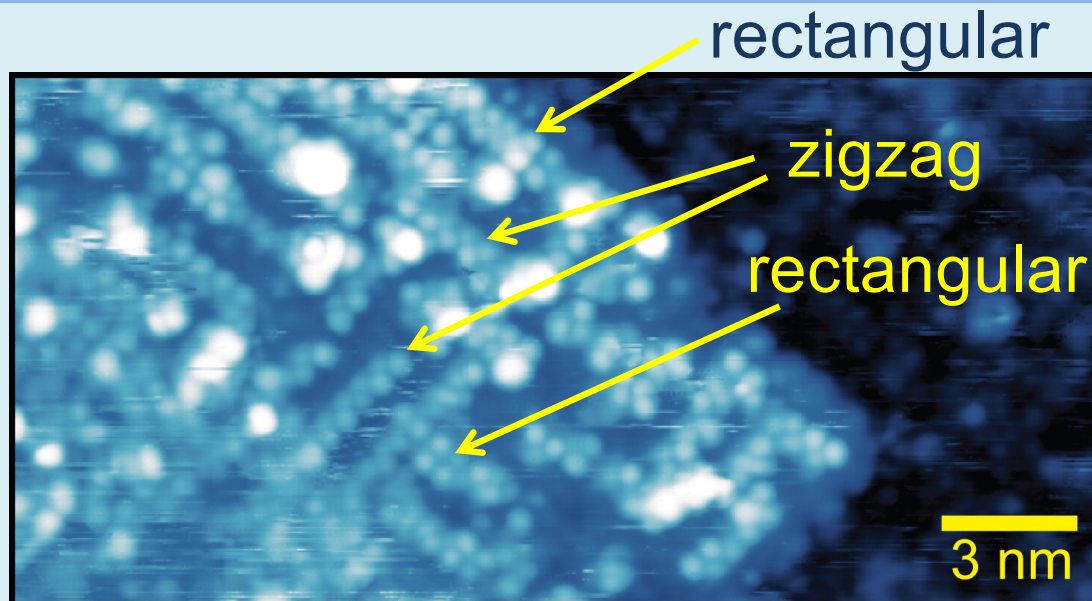
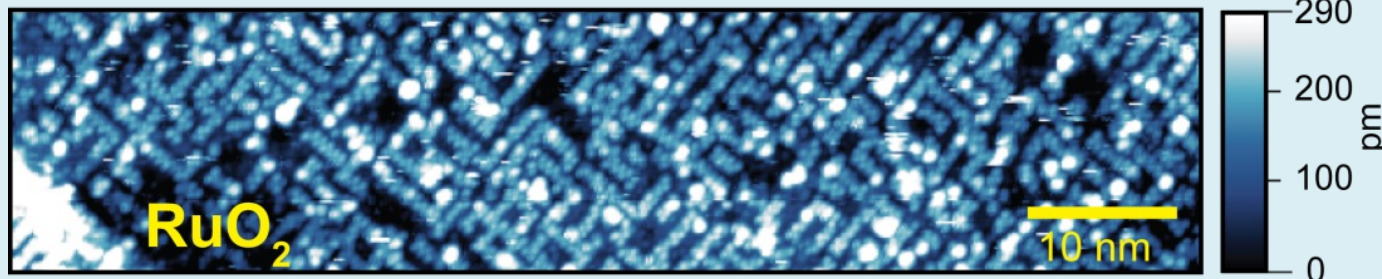
ex-situ AFM (topography)



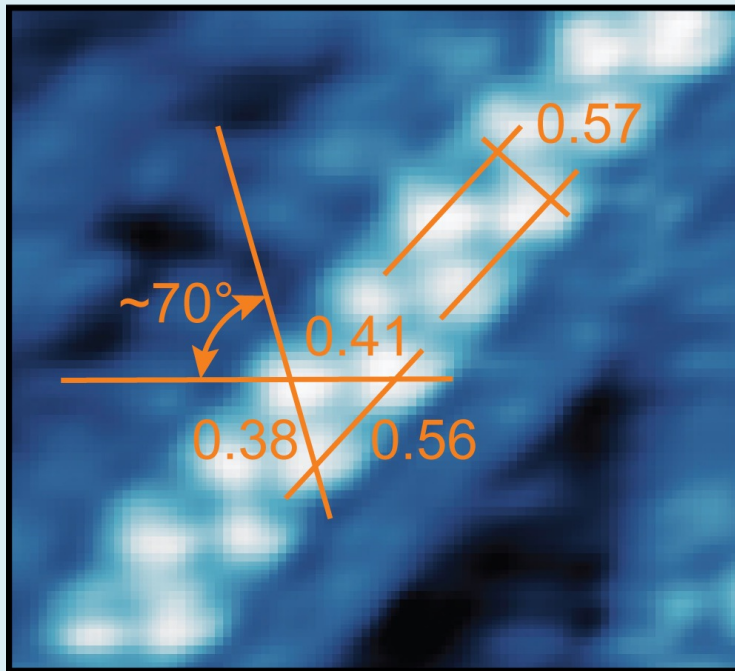
in-situ STM



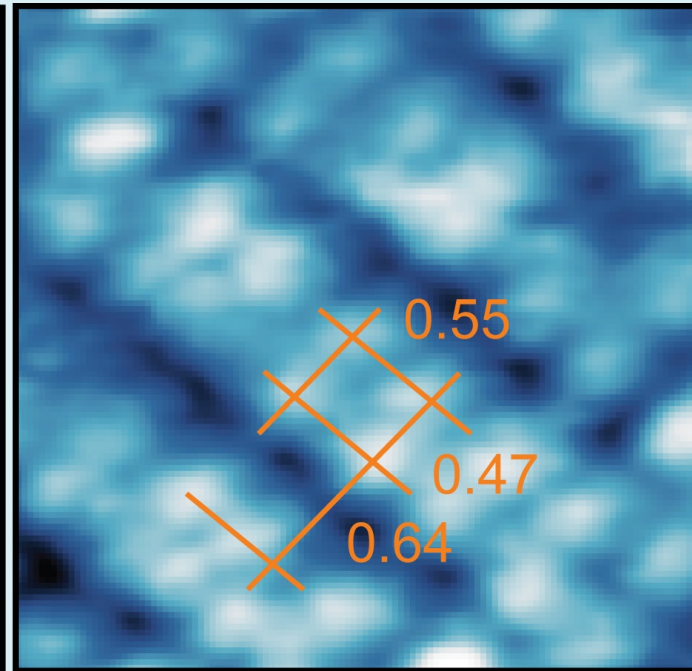
Competing surface patterns



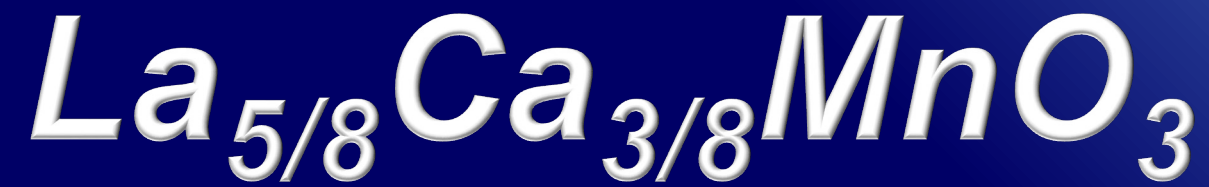
Zigzag and rectangular patterns



zigzag



rectangular

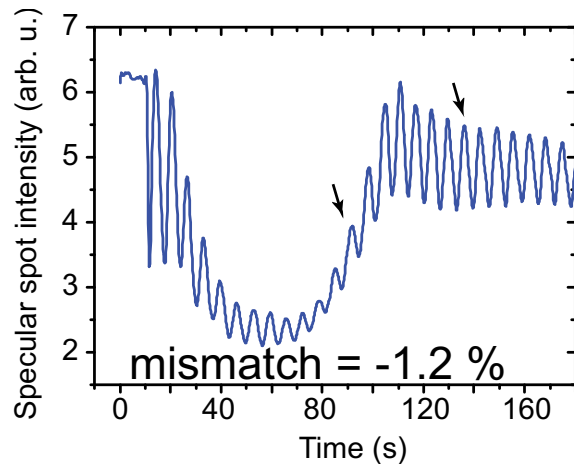


Classical *Colossal magnetoresistance* material

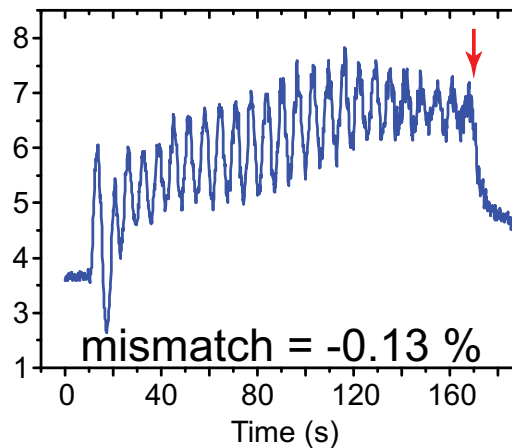
Growth dynamics vs. conditions

Growth behavior strongly depends on the substrate and relatively small variations of oxygen pressure.

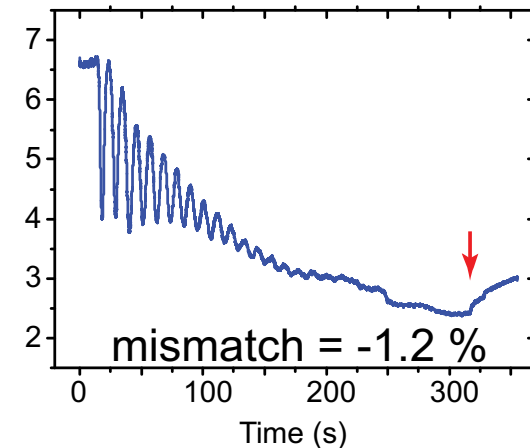
SrTiO₃(001), 50 mTorr



NbGaO₃(110), 50 mTorr

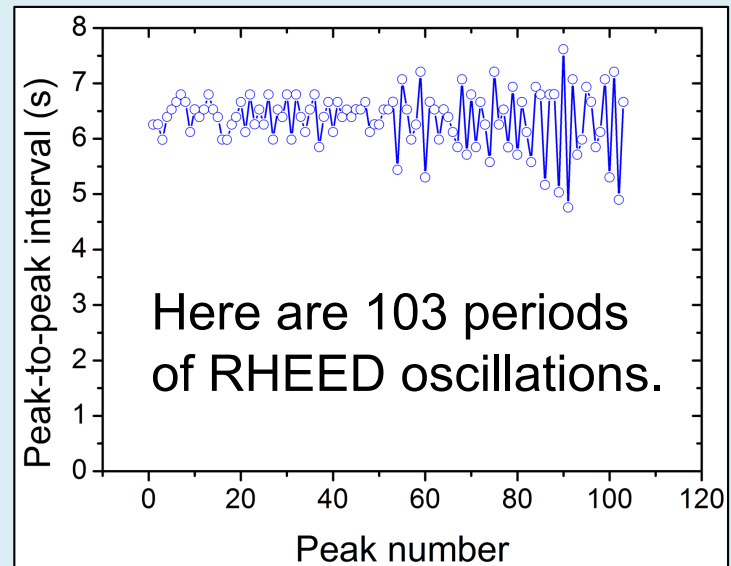
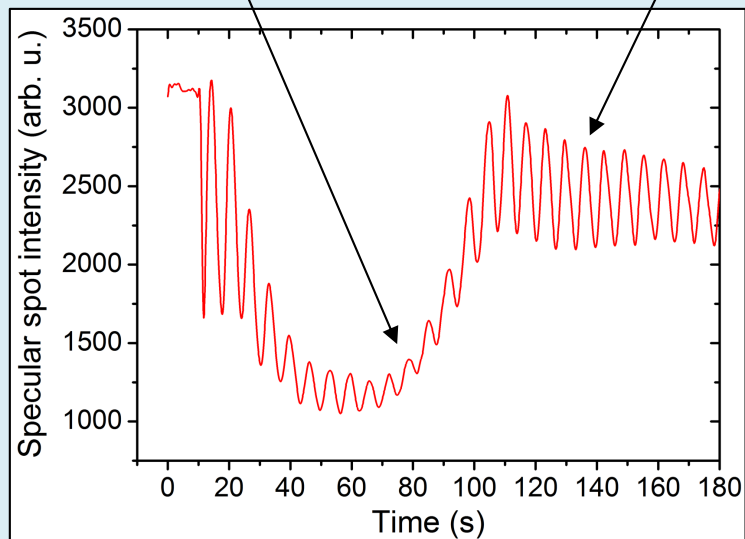
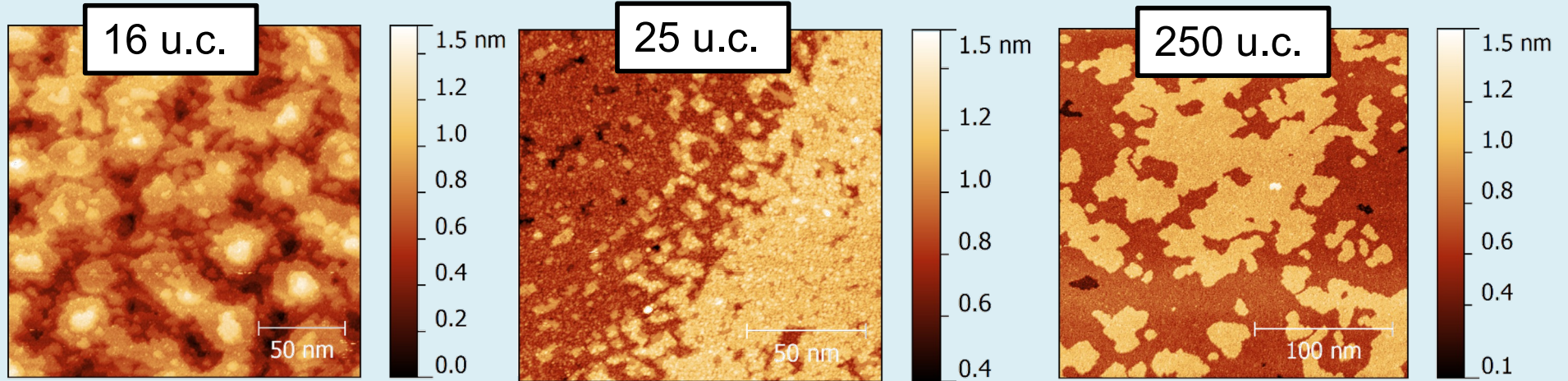


SrTiO₃(001), 20 mTorr

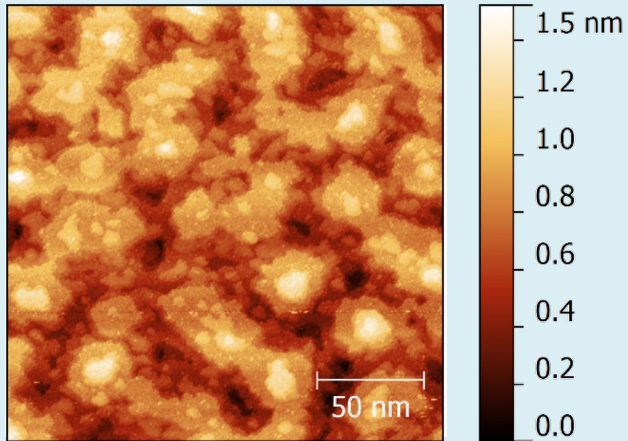


$T_s = 750 \text{ }^\circ\text{C}$

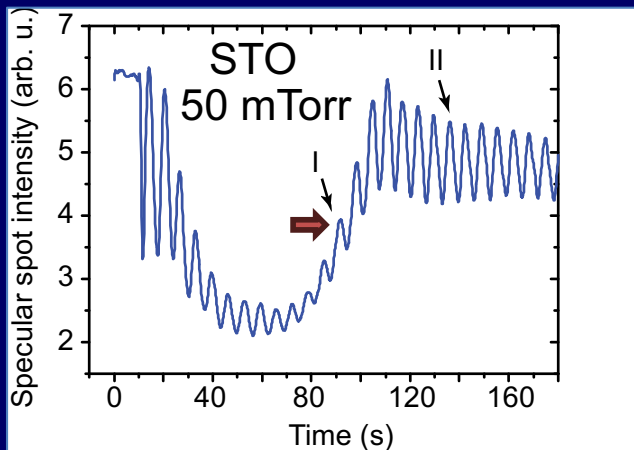
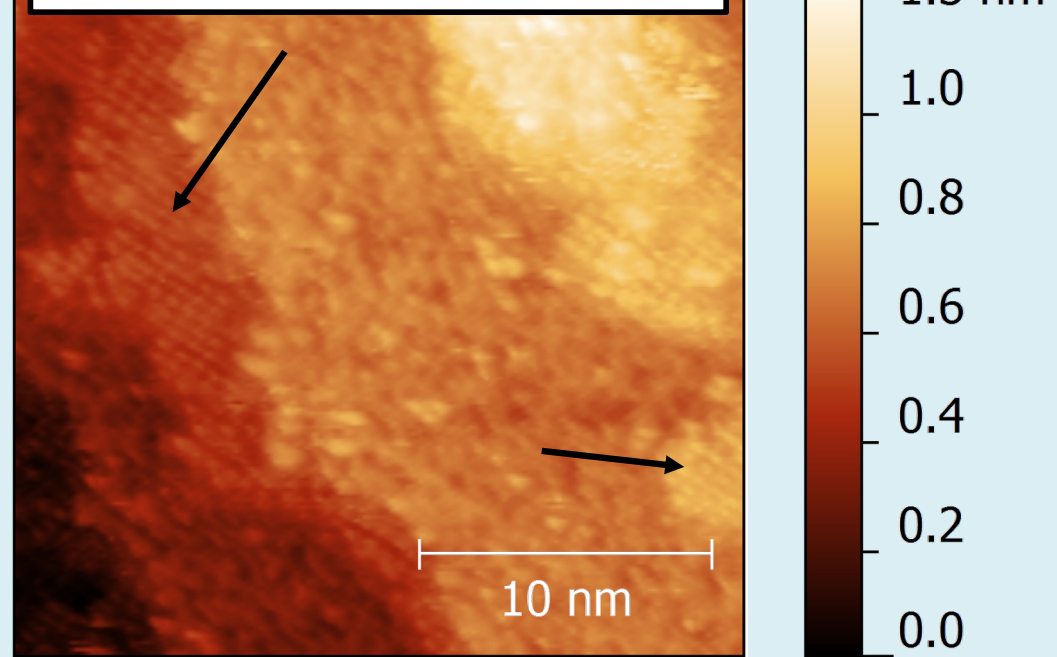
Evolution of surface morphology



16 u.c. on SrTiO₃



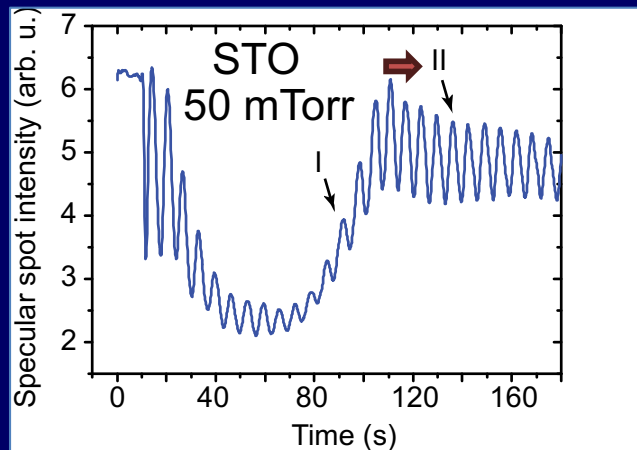
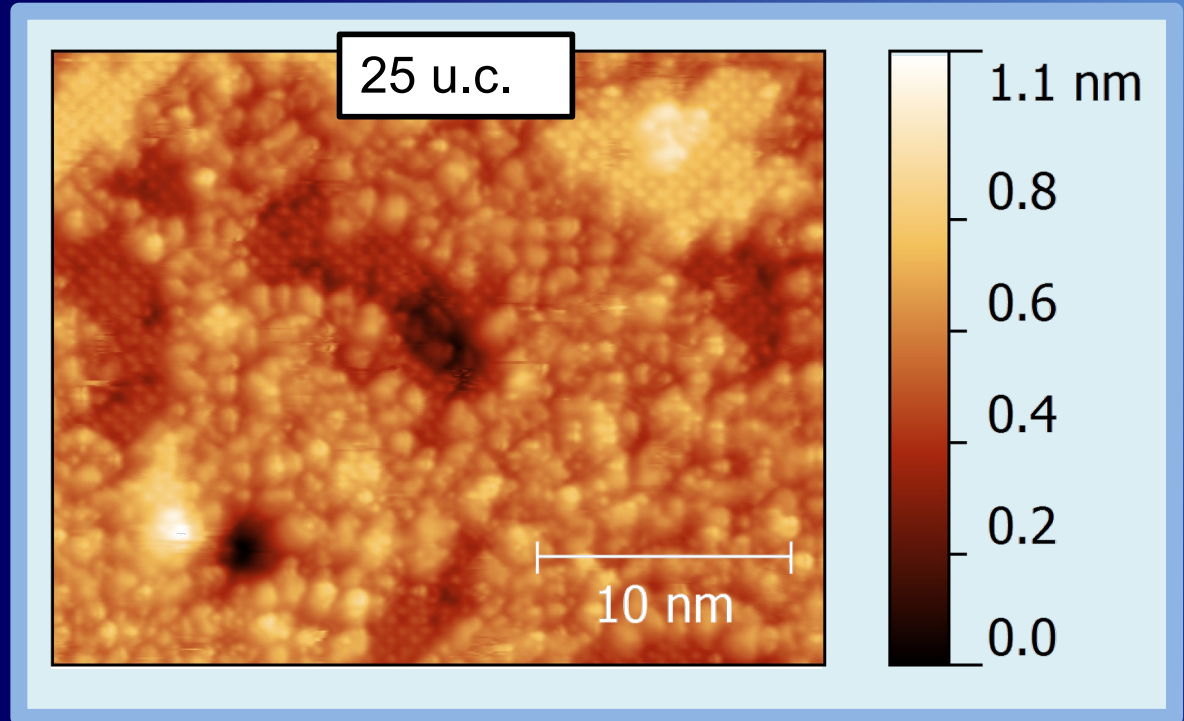
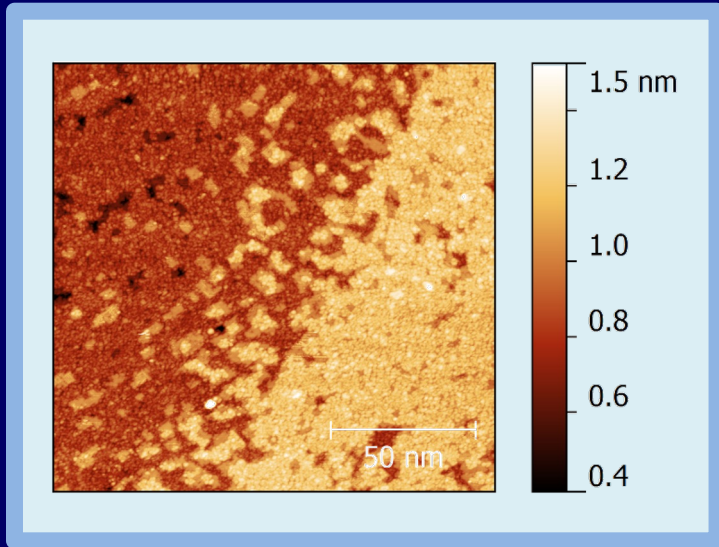
$(\sqrt{2} \times \sqrt{2})R45^\circ$ reconstruction



- Up to 7 u.c. layers can be seen
- Two terminations - *ordered* and *disordered*

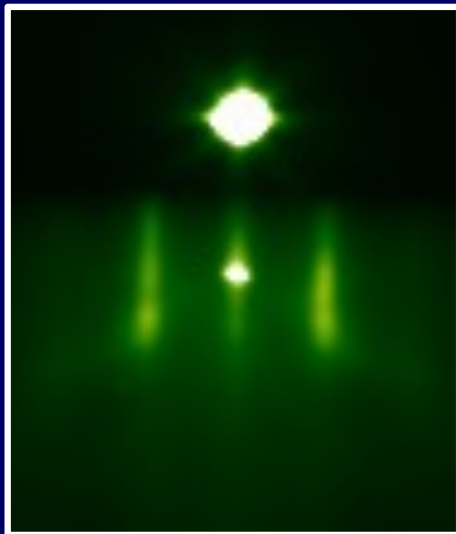
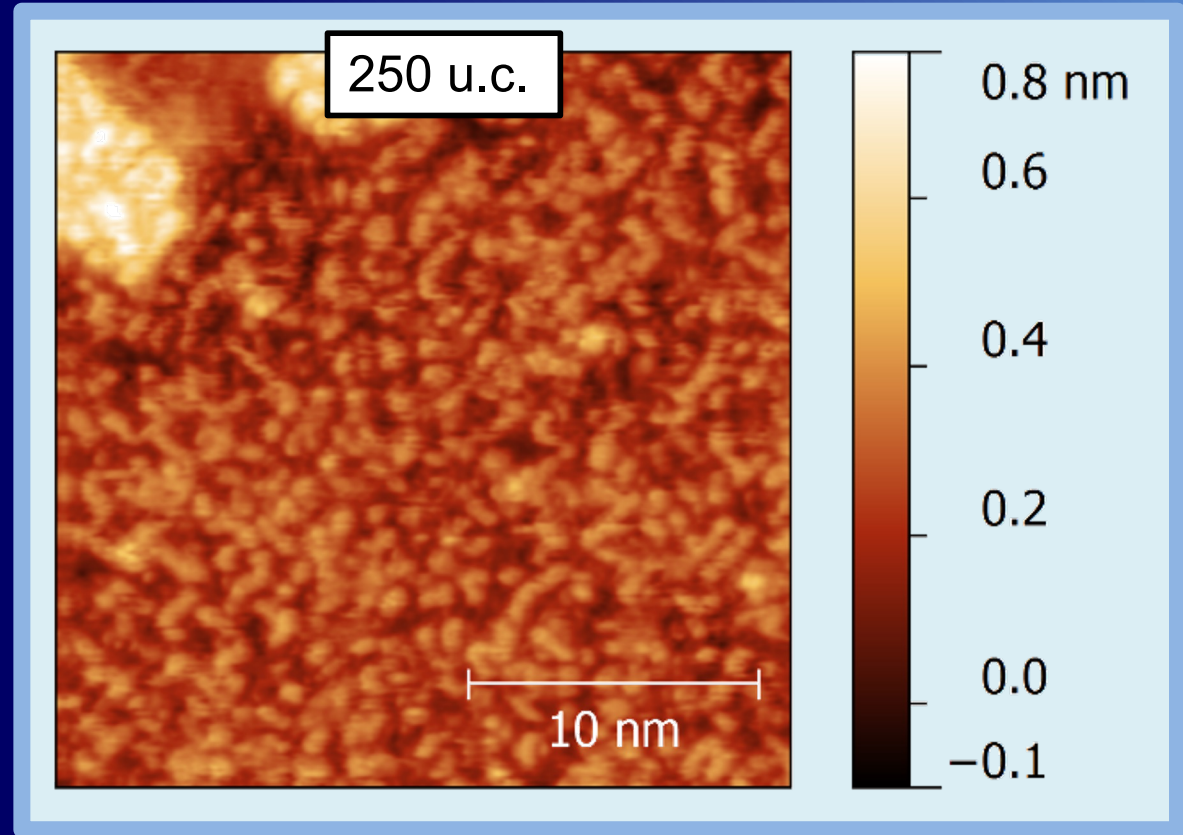
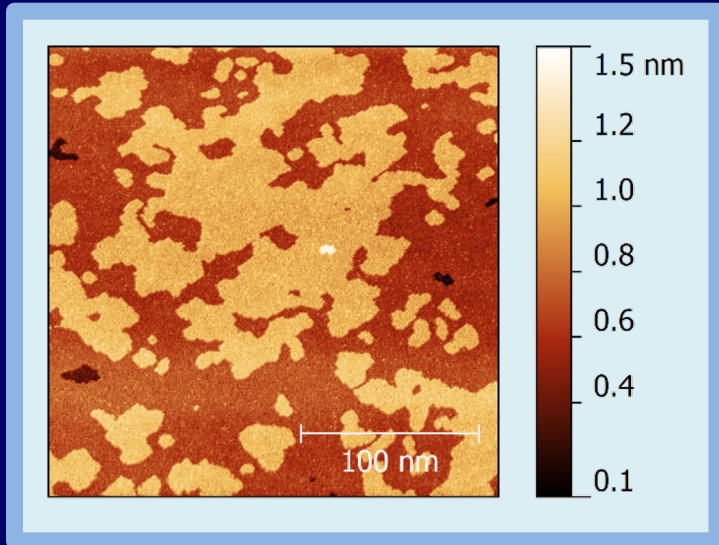
$$V_t = -1.8 \text{ V}, I_t = 40\text{-}90 \text{ pA}, T = 297 \text{ K}$$

25 u.c. on SrTiO₃



- Larger islands
- Up to 3 u.c. layers can be seen
- Two terminations: *ordered* and *disordered*.

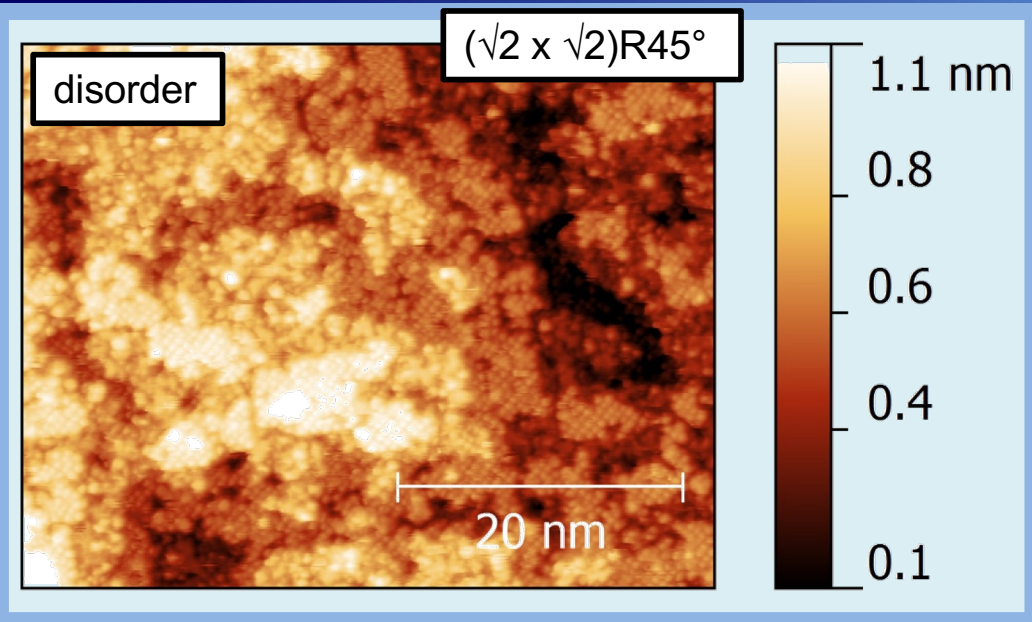
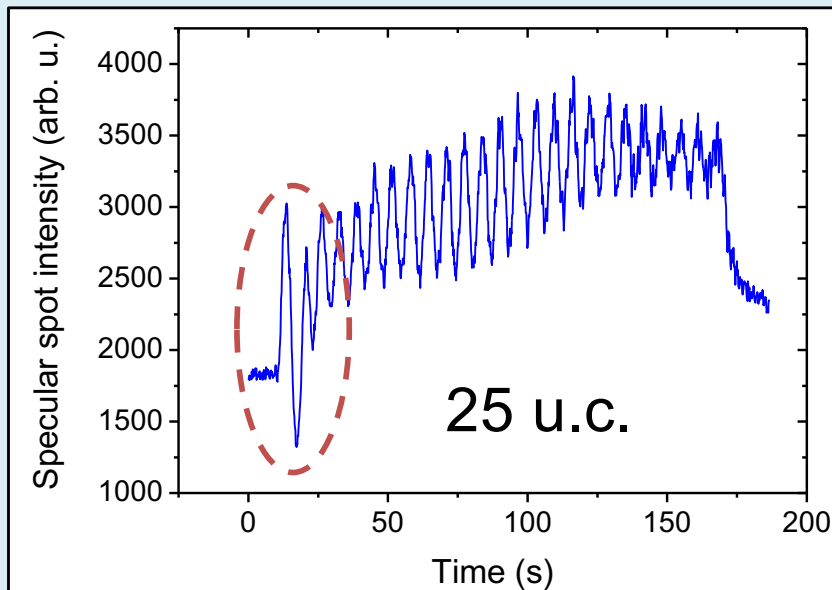
250 u.c. on SrTiO₃



- Up to 3 u.c. layers can be seen
- One termination - *disordered*
- Nearly perfect layer-by-layer growth

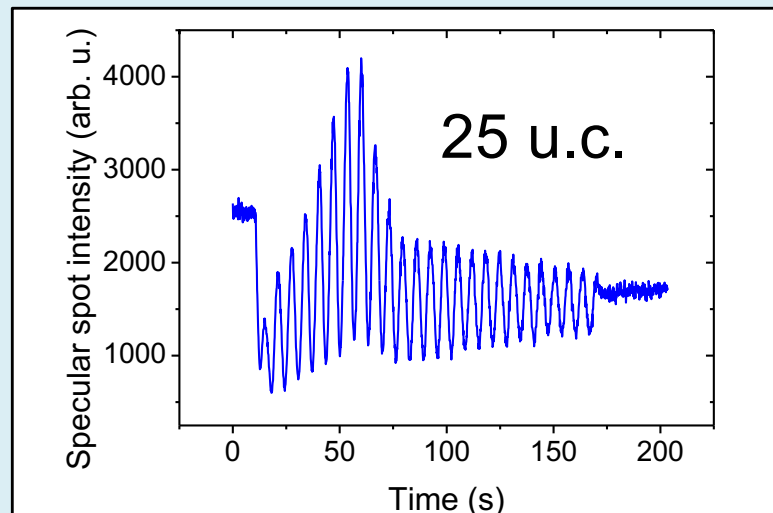
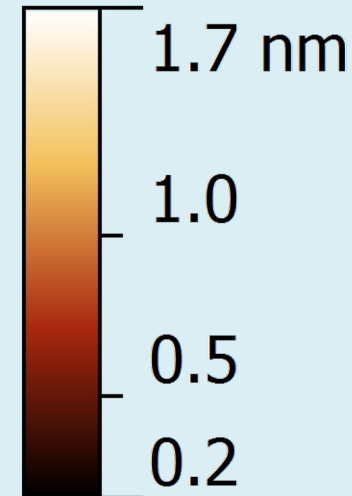
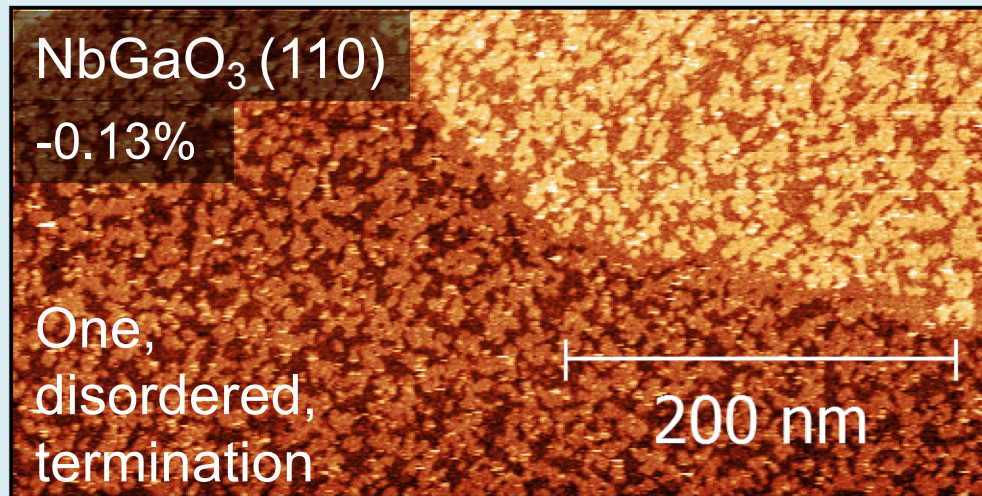
Stable layer-by-layer growth on A/B-terminated NGO substrates

NbGaO₃ (110), lattice mismatch -0.13%



- The surface is doubly-terminated.
- A and B terminations are approximately equally present.

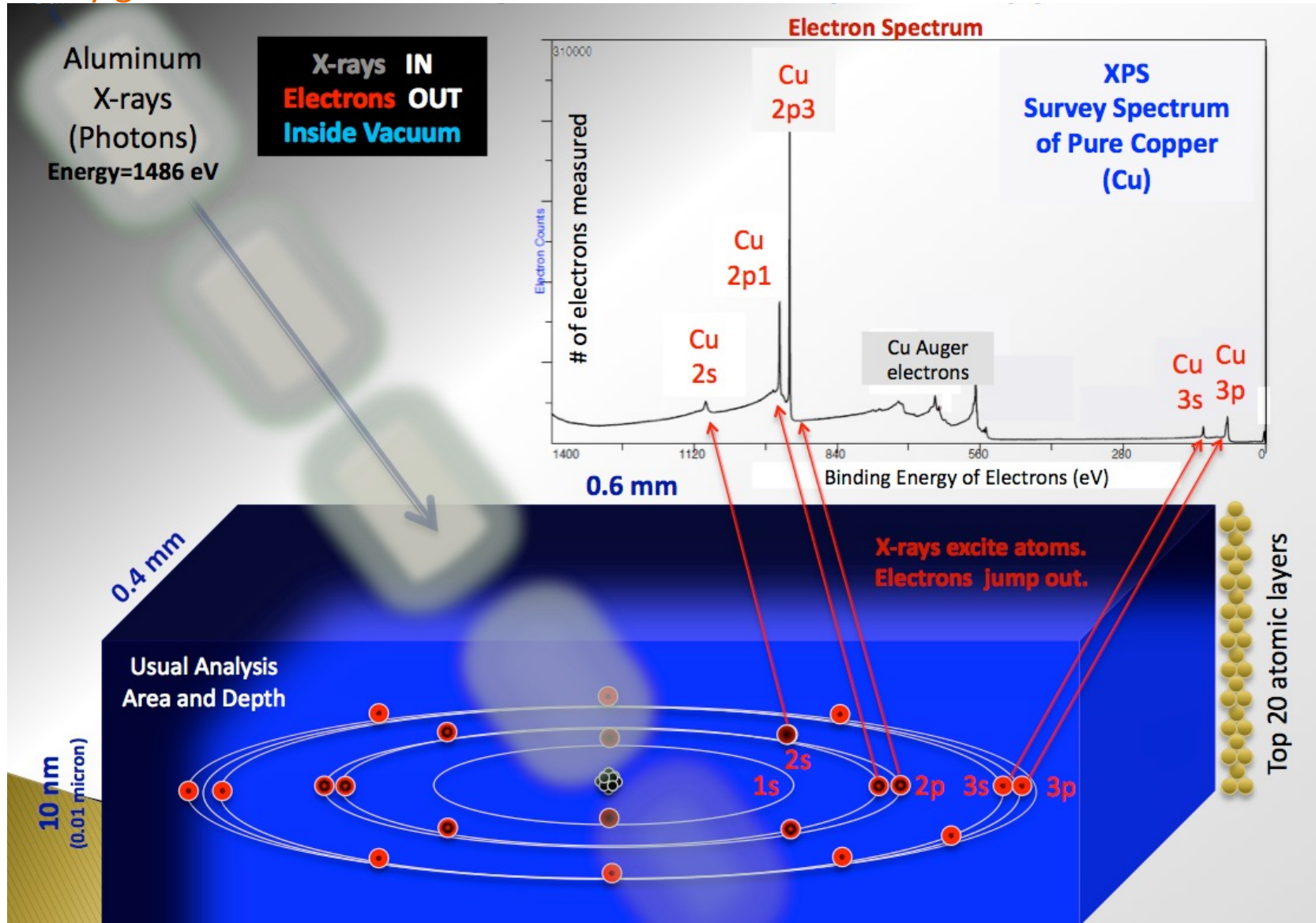
25 u.c. on B-terminated NGO substrate – single termination



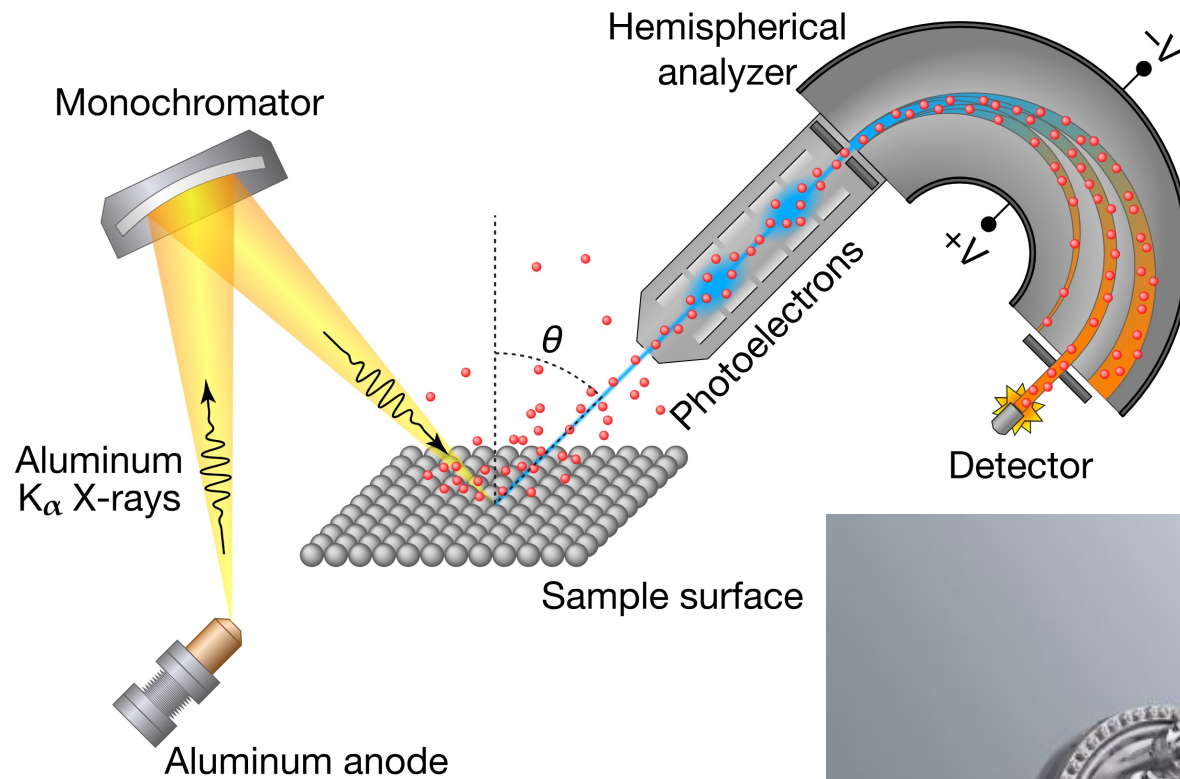
- The surface is single-terminated
- The termination is disordered, =>
- ***Disordered termination is B-termination***

XPS: X-ray Photo-electron Spectroscopy

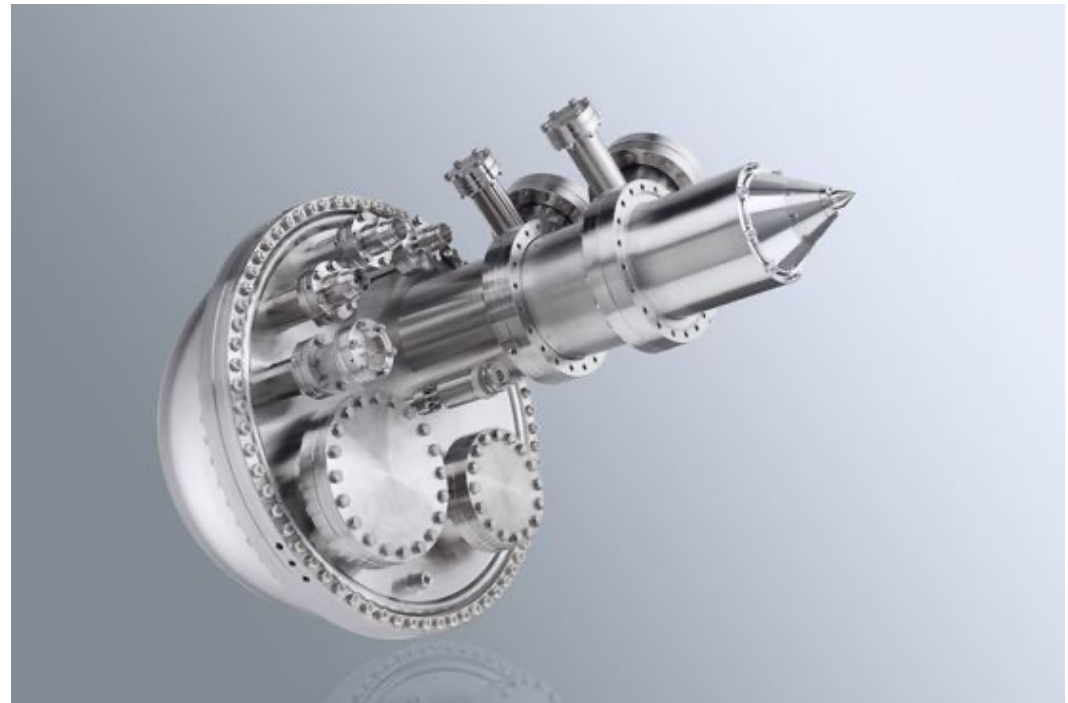
X-ray gun



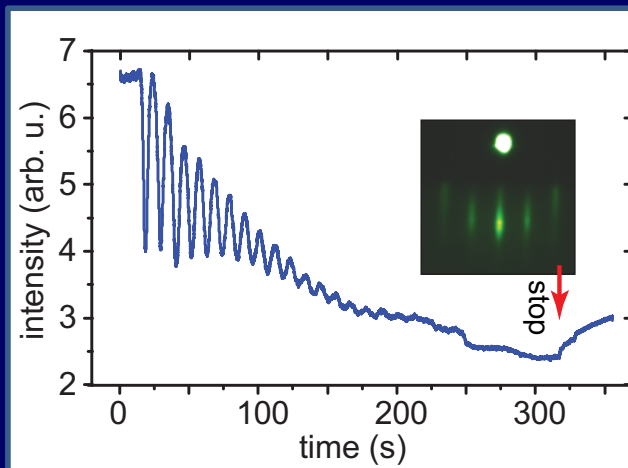
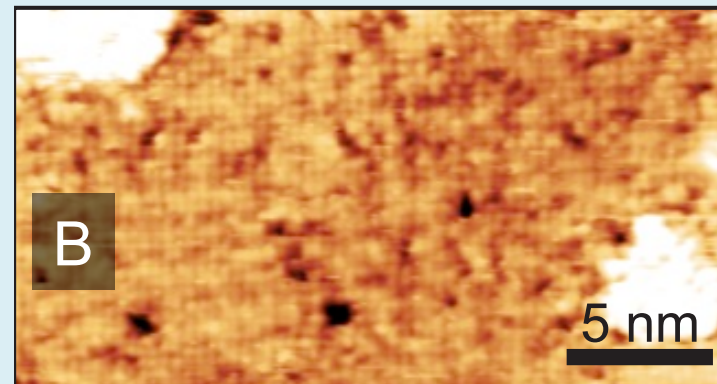
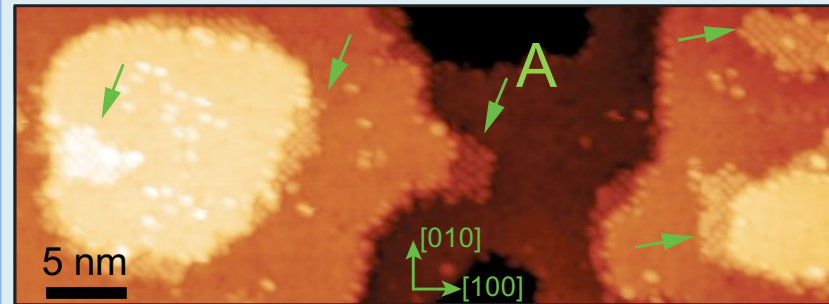
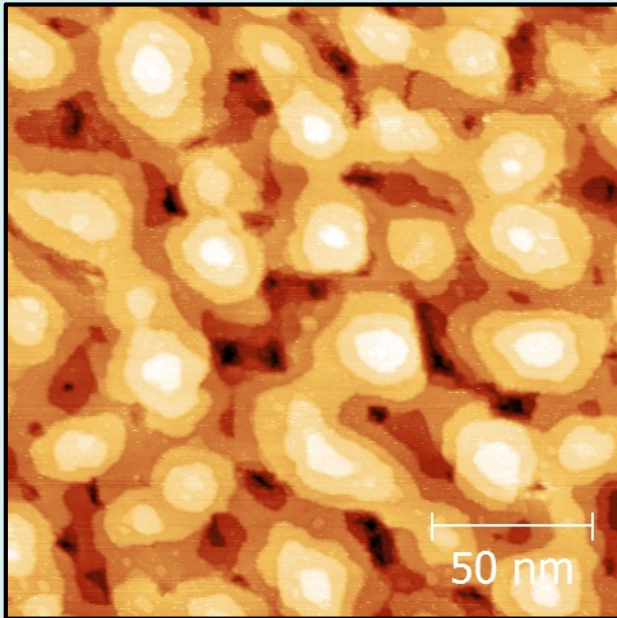
XPS: X-ray Photo-electron Spectroscopy



<https://grimmgroup.net/research/xps/background/>

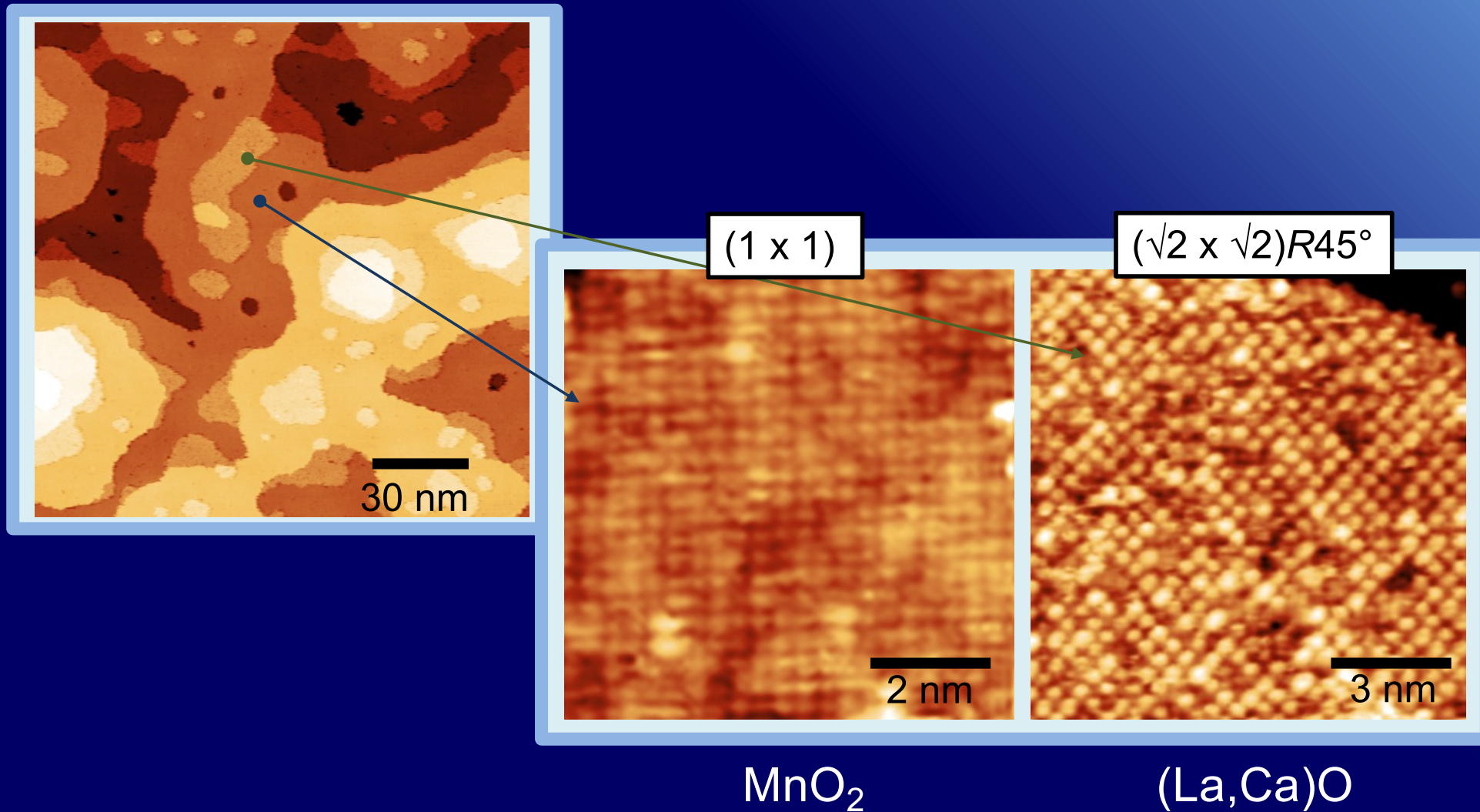


Terminations: Mounded structure

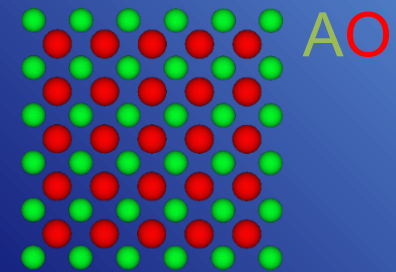
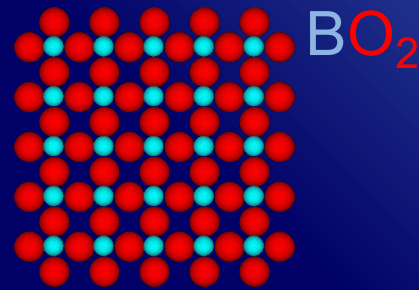
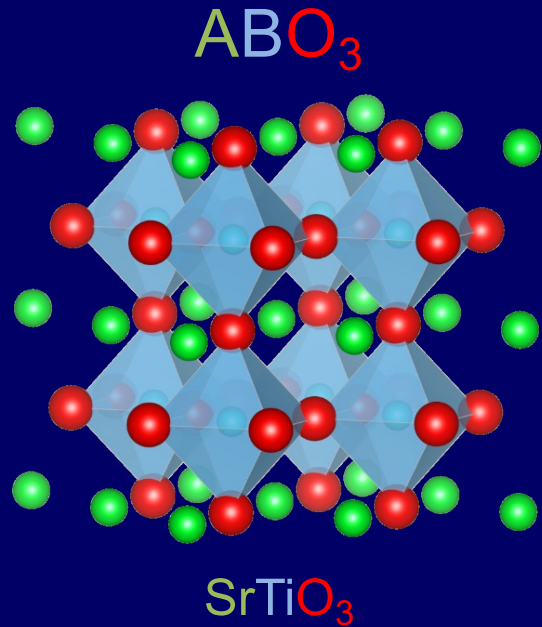


- A: $(\text{La,Ca})\text{O}$
- B: MnO_2

High-resolution images

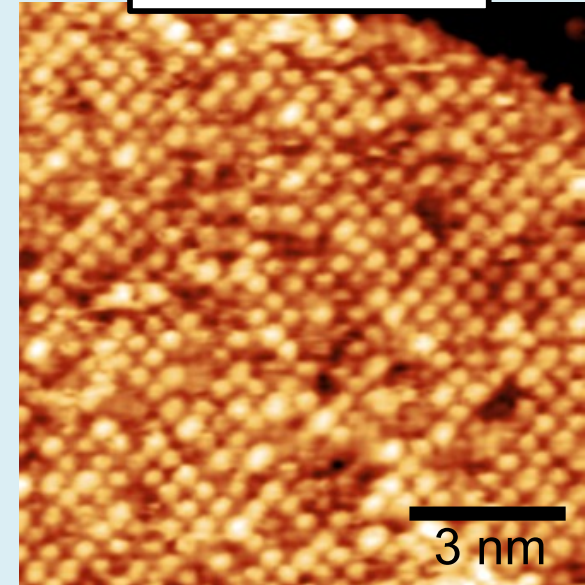
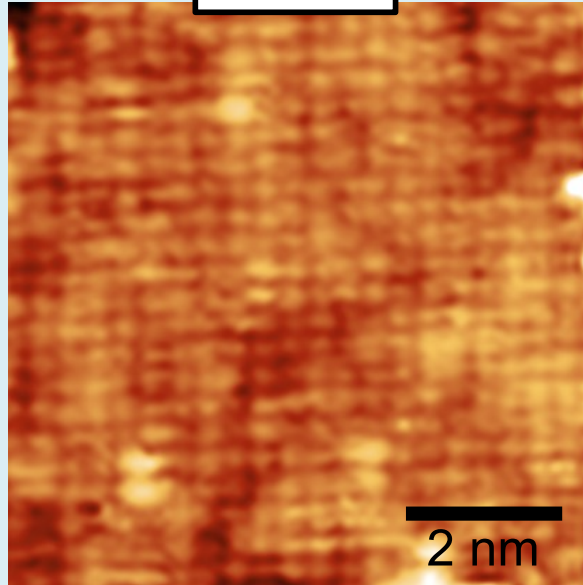


Meaning of the patterns



(1×1)

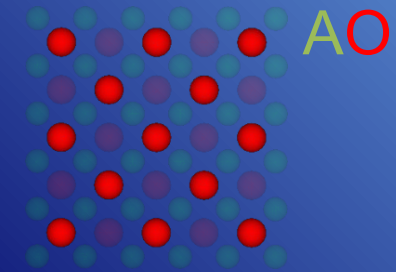
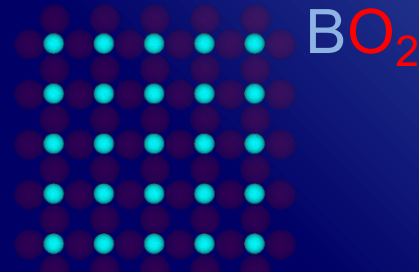
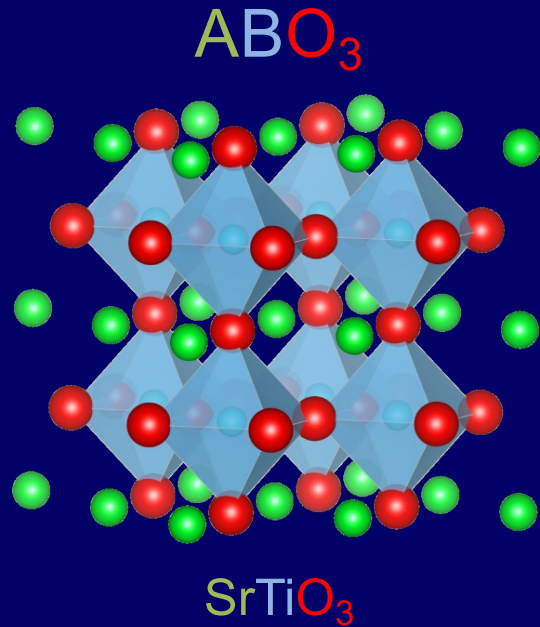
$(\sqrt{2} \times \sqrt{2})R45^\circ$



MnO_2

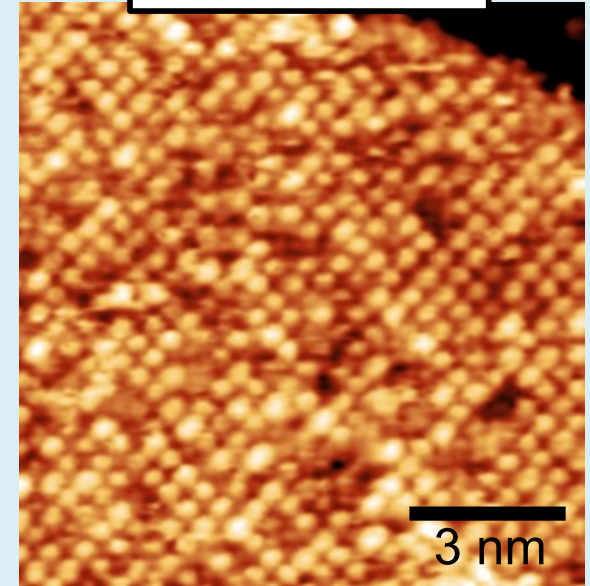
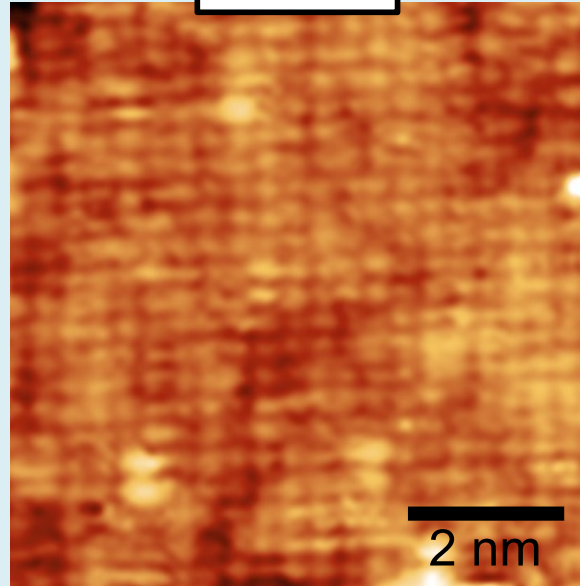
$(La,Ca)O$

Meaning of the patterns



(1×1)

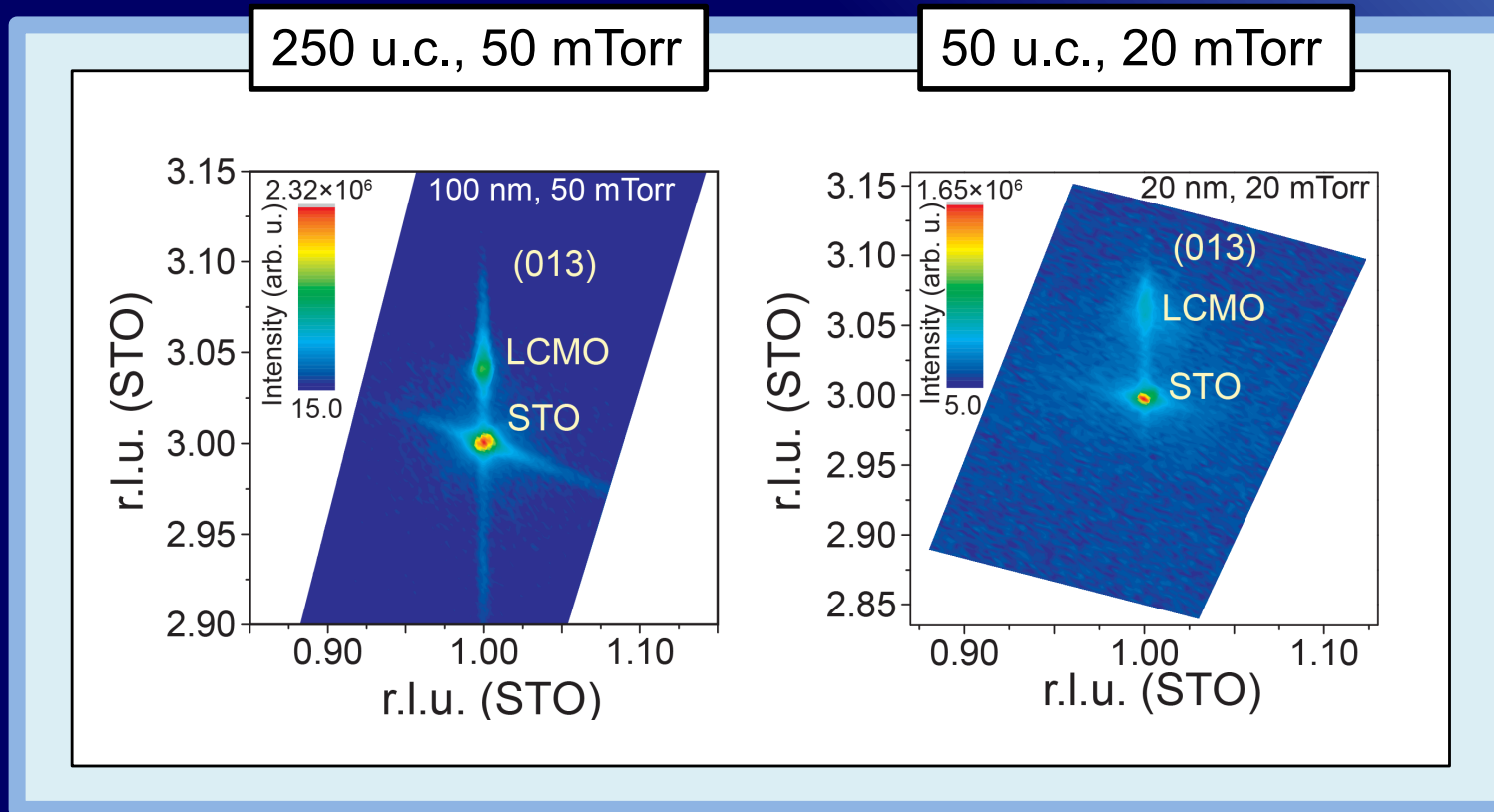
$(\sqrt{2} \times \sqrt{2})R45^\circ$



MnO_2

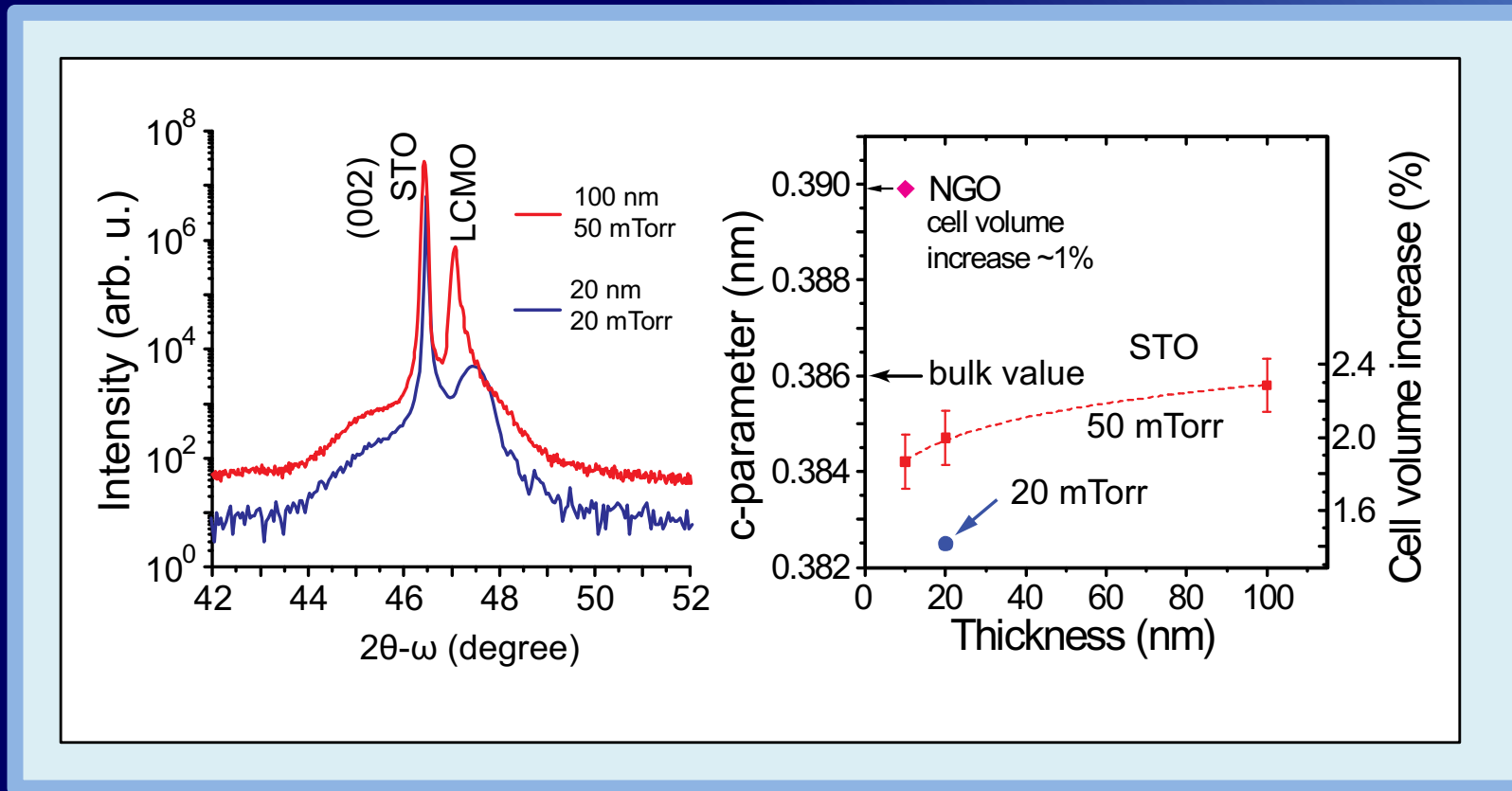
$(La,Ca)O$

XRD: q-space maps



All films are coherently strained to the substrate in plane

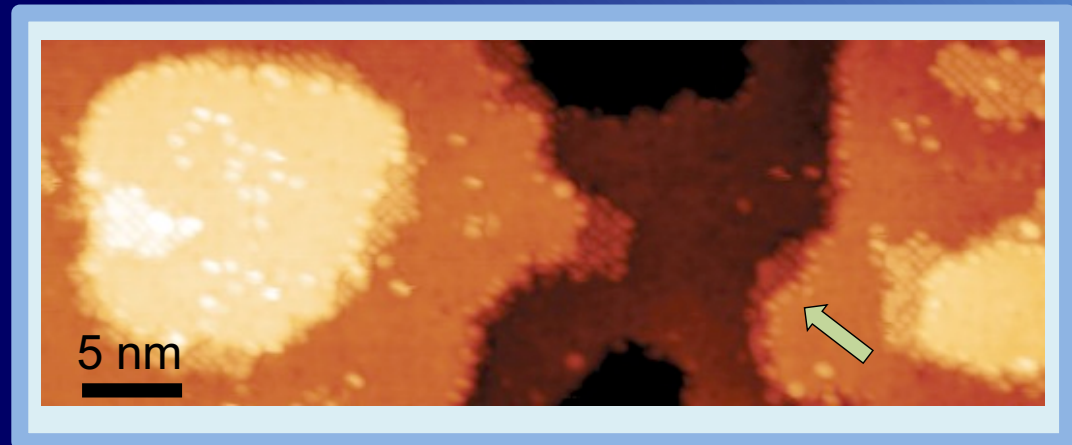
Out-of-plane lattice parameter



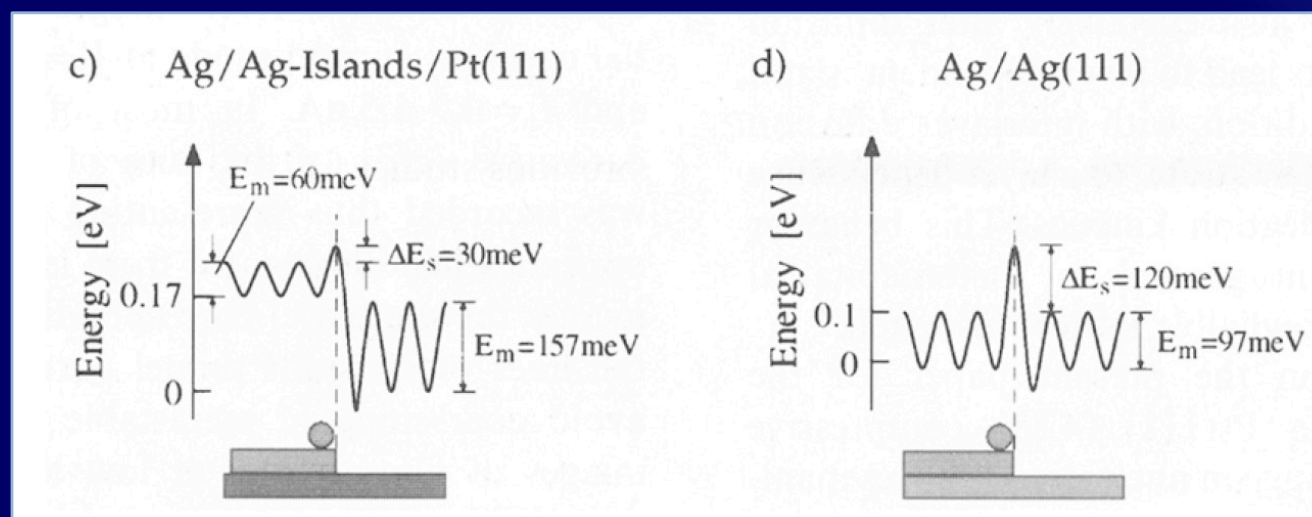
- 50 mTorr: out-of-plane lattice parameter increases with thickness
- 20 mTorr: film lattice is noticeably more compressed out-of-plane

Interpretation of the growth evolution

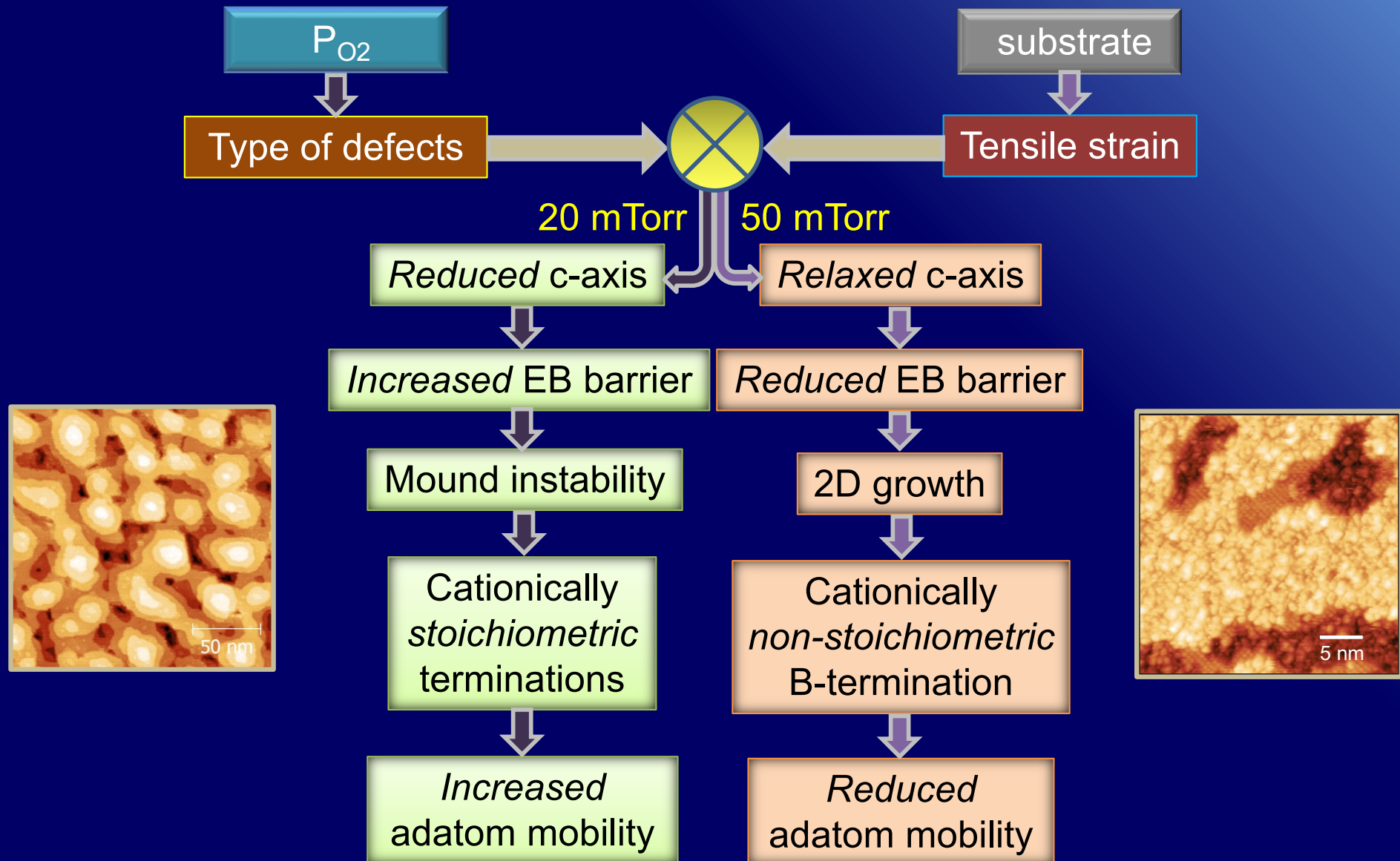
- Dependence of the barrier for interlayer adatom transport (Ehrlich-Schwoebel barrier) on strain.



Ag-on-Pt (111) as an example

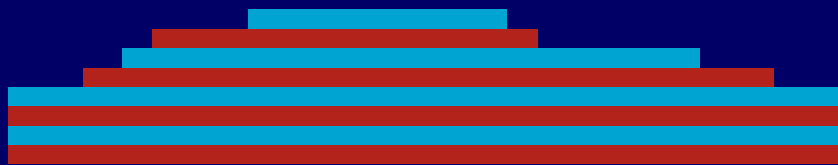


Cause-effect relationships

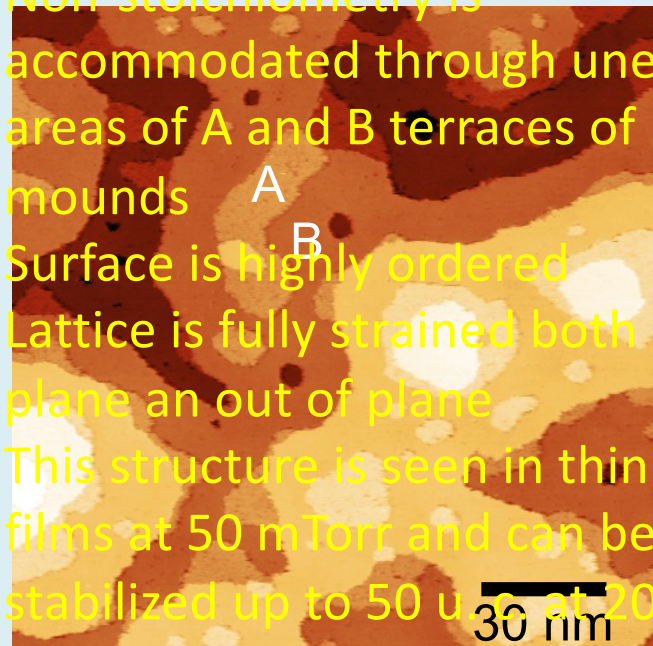


Film structure models

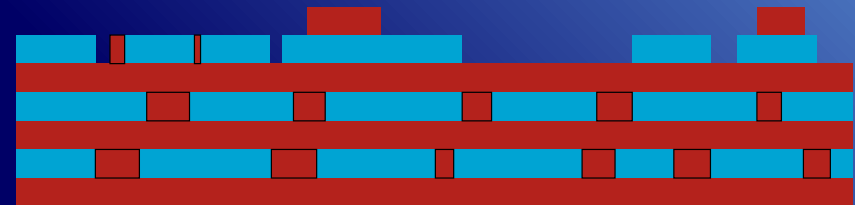
Mounded structure



- Non-stoichiometry is accommodated through unequal areas of A and B terraces of mounds
- Surface is highly ordered
- Lattice is fully strained both in plane and out of plane
- This structure is seen in thin films at 50 mTorr and can be stabilized up to 50 u. c. at 20 mTorr



Layer-by-layer growth



- Non-stoichiometry is accommodated via anti-site cation defects in the B sublattice
- Surface is disordered
- Lattice expands in the out-of-plane direction
- This structure is seen in all films >25 u. c. at 50 mTorr
- Apparent adatom mobility increases with increasing thickness

